



TOMBO Workshop

ACCMS 7 in Suranaree University of Technology
Nakhon Ratchasima, Thailand

23-24 July 2013

Recently, First-principles calculations have been used not only in materials science but also in industrial researches, and has become very popular. However, there is a question whether the calculations are correctly performed to be compared with experiments and to design or predict new materials on the basis of the correct understanding of the basic theories behind the complicated calculation algorithms. Although the basic equation, i.e., quantum mechanical Schrödinger equation or Dirac equation for the component particles of electrons and nuclei is known, and nuclei may be treated approximately as classical particles with point charge, it is impossible to treat the system exactly except for the simplest system of an isolated hydrogen atom. Within the limited resource of the computational power, even if we use huge supercomputer, somewhat crude approximation must be made in the first-principles calculation. Therefore, it is required for us computational materials scientists to clarify what we can do and what we cannot do, and to develop a new program as accurate as possible and to show the way to apply it appropriately.

The Hartree-Fock approximation is an accurate approximation in a sense that it correctly includes exchange interaction between electrons, satisfies virial theorem, the Pauli principle, and the conservation laws. However, the interactions which is not included in the Hartree-Fock approximation are called electron correlations are generally not negligible at all, and sometimes become quite important in various physical and chemical phenomena and attract great interest of many researchers. The configuration interaction (CI) method to incorporate the effect of electron correlations is accurate but its application is limited to rather small systems only, because it requires vast amount of computational resources if the system becomes large. Therefore, as a standard first-principles method, one invokes density functional theory discovered by Hohenberg and Kohn. In this theory, for nondegenerate ground state, the original equation for the $3N$ -dimensional degrees of freedom for the N -electron system becomes a simple equation for the 3-dimensional degrees of freedom. However, explicit form of an exchange-correlation interaction applicable to general problems is not known, although first the local density approximation (LDA) was introduced on the basis of electron-gas model by Kohn and Sham, and then it is extended to the local spin density approximation (LSDA). Then various forms of the generalized gradient approximation (GGA), LDA+ U , and hybrid methods have been proposed so far. However, the problem occurs when the result of the ground state theory DFT is compared with experiments. These approximate exchange-correlation interactions have several arbitrary parameters, which are chosen so as to fit the results to the experiments. For example, the parameter U is determined so as to fit to the experimental band gap. The hybrid models combine the LDA that underestimates the band gap and the Hartree-Fock approximation that overestimates the band gap to fit to the experimental band gap. Then the virial ratio, which should be exactly equal to -2 for accurate calculation, becomes far off the ideal value. We have developed TOMBO to determine absolute values of energies around Fermi level since 20 years ago, and adopted

the *GW* approximation as a one accurate method. The characteristics of TOMBO is not to pseudopotentials but to describe all electrons by means of a combination of atomic orbitals (AOs) and plane waves (PWs). Therefore, it is possible to determine absolute energies, and, eventually by using the *GW* approximation, not only the ionization potential, electron affinity and energy gap, but also all excitation spectra at once in a single calculation. TOMBO can accurately describe the core electron states, and therefore we have succeeded in an accurate determination of the hyperfine structure constant. Using the similar advantage of the method, we have also succeeded in a series of the simulations of foreign atom insertion into fullerenes, and it is our pleasure that this investigation could lead to a significant information to experimentalists. And in the TDDFT electron excited-state dynamics simulation, we have clarified the elementary process of electron transfer in very short time, which is very hard to observe experimentally.

Recent progress (under development) is the implementation of electron conductivity by transforming plane waves, which is capable to describe continuum states, to localized Wannier functions as well as originally localized atomic orbitals, the calculation of the coefficient of the van der Waals interaction by calculating polarization of atoms accurately, the thermal conductivity calculation and the design of thermoelectric devices by the evaluation of the 3rd and 4th order derivative of the total energy with respect to the atomic coordinates, precise calculation of the NMR chemical shift, and so on.

In first-principles calculations, their computational amount is always a serious problem. Even supercomputer does not have infinite memory, and has only limited speed of computation. In recent years, the CPU clock speed has not increased from 2-3 GHz, the tips became extremely complicated due to downsizing to several tens of nano meter scale, and every machine has four-layer structure composed of core, CPU, node, and system.

Automatic vectorization and parallelization of Fortran programs supported 20 years ago are no more expected in general, and, in order to speed up the program, it became inevitable for our scientists to make the program parallelized by using MPI. In TOMBO, we have achieved MPI parallelization since 10 years ago, although it is not easy to distribute memory in the DFT calculation. However, in *GW* calculation, the parallel efficiency is quite high, and, for some target systems, *GW* calculation can be performed within the same wall clock time period needed to the DFT calculation. In what follows, we will explain the detailed algorithm and characteristics of TOMBO.

Since the development of TOMBO code is still under progress, we would appreciate it very much if you could give us your opinions and comments of TOMBO. We also appreciate your questions of using TOMBO. We hope that TOMBO will be used in various applications in the future. With your help, we would like to work on further improvements and implementations of new functions in TOMBO.

23-24 July 2013
TOMBO group

1 Preface

Density functional theory (DFT)[1] and its local density approximation (LDA)[2] have been used in great many electronic structure calculations and first-principles molecular dynamics simulations. There are many approaches in the electronic structure calculations within the local density approximation in density functional theory.

Among them, the pseudopotential approach combined with plane wave (PW) expansions has been applied to the *ab-initio* molecular dynamics (MD) simulations with reasonably high accuracy. However, it is difficult to treat phenomena (hyperfine interaction, XPS, Xanes, etc.) related to core electrons by this method. One problem in generating good pseudo potentials is related to the fact that the core contribution to the exchange-correlation potential is not simply an additive quantity. Moreover, it is not easy to create efficient pseudopotentials, which require only small number of plane waves. For example, first-row elements from B to F have very localized 2p valence orbitals and transition-metal elements have also very localized 3d valence orbitals in order to screen the strong Coulomb potential of the ions. This spatial locality of 2p and 3d orbitals is caused from the fact that there is no inner 1p and 2d orbitals to which the 2p and 3d orbitals are orthogonal in radial. Furthermore, it is not easy to treat ionization process of hydrogen atoms by using a pseudopotential approach.

On the other hand, linear combination of atomic orbitals (LCAO) approaches can enable us to treat all electrons. However, these methods have an intrinsic problem of incomplete basis set, and therefore there is a problem in applying them in perturbation theory or spectral expansion, which requires a description in the complete Hilbert space. It is also difficult to consider a negative affinity problem by these methods. Related but slightly different problem inherent to these methods is a basis set superposition error (BSSE). There is also some trouble in the Gaussian basis method to describe cusp in the wave-function at the nuclear position.

The methods using muffin-tin approximation such as APW and KKR are also all-electron methods but powerful dense periodic systems only. They cannot be easily applied to the systems with surfaces or vacuum region.

In these respects, it is highly desirable to develop new method, which combines the PW expansion technique with the LCAO technique to remove pseudopotentials in the PW expansion methods and to make the basis set complete in the LCAO methods. This is the main idea to introduce the all-electron mixed basis approach. TOMBO is the program package using this approach. Therefore, TOMBO is the all-electron first-principles method, which can be applicable to both isolated and periodic systems with complete basis set. It is not the overcomplete basis set because only limited number of PWs is used in the computation.

The powerfulness of TOMBO is not only based on these features but also based on

the fact that it enables us to perform the state-of-the-art calculations such as GW approximation and Bether–Salpeter equation. Using these methods, TOMBO can treat the problems related to electron correlations, electronic structure around the band gap, excitation spectra, and so forth.

The “mixed-basis approach” indicates the method using both plane waves and Bloch sums made of atomic orbitals as the basis set. Historically, Louie, Ho and Cohen introduced Gaussian atomic orbitals in the pseudopotential PW approach to treat transition metal crystals with relatively small number of PWs [3]. Concerning the mixed-basis approach, Ho et al. presented a formulation of the force acting on nuclei [4, 5]. It includes Pulay force. However, this was not the all-electron calculation. It is a simple idea to extend this approach to the all-electron calculations. Instead of using Gaussian-type orbitals, TOMBO uses numerical AOs, which makes possible to describe the correct cusp behavior in the all-electron calculation. TOMBO confines all AOs inside the non-overlapping atomic spheres. This makes unnecessary to compute very complicated overlap integrals between AOs centered at adjacent atoms, and simultaneously reduce the problem of overcompleteness, because the confined AOs are clearly more localized than the original AOs and have less overlap with PWs.

To do the first-principles molecular dynamics simulation, we use Born–Oppenheimer (BO)’s adiabatic approximation by assuming nuclear mass is much larger than the electron mass. Under this assumption, for the force exerting on atoms, we have to calculate the variational force due to the fact that AOs depend explicitly on the atomic positions, in addition to the usual Hellmann–Feynman force. In the force calculation, we use the same method introduced by Ho et al. [4, 5].

The all-electron mixed basis approach has the following advantages:

- (1) The number of basis functions can be significantly reduced. For example, for carbon systems, first-principles MD can be performed with 7 Ry cutoff energy of PWs. In contrast, standard pseudopotential approaches requires 40 Ry cutoff energy of PWs.
- (2) In Hamiltonian matrix elements, it is not necessary to store PW-PW part because it is given simply by the Fourier components $V(\mathbf{G} - \mathbf{G}')$.
- (3) It is possible to accurately treat core states because we determine AOs by using Herman–Skillman code with logarithmic radial mesh.
- (4) There is no complexity to generate and treat pseudopotentials. There is also no problem of transferability.
- (5) The overlap between AOs and PWs is calculated accurately by first performing angular integral analytically and then performing radial integral of spherical Bessel functions numerically in logarithmic radial mesh.

- (6) Because AOs are confined inside non-overlapping atomic spheres, there is no BSSE problem, and it is not necessary to calculate overlap integrals between AOs centered at different atoms, which might produce unnecessary computational errors. Simultaneously, this reduces the overcompleteness problem.

In Kawazoe's Lab. in Inst. Mater. Res. (IMR), Tohoku Univ., Maruyama (now Adv. Indust. Sci. Tech. (AIST), Nagoya) and Ohno (now Yokohama Nat. Univ. (YNU), Yokohama) developed all-electron mixed basis program using numerical AOs and succeeded in a first-principles MD simulation both for spin-unpolarized systems and for spin-polarized systems. A part of this work is written in the Dr. thesis of Maruyama. Then Ohno performed first-principles MD simulations of foreign atom insertion into fullerene [8–10], and implemented diamagnetic susceptibility of semiconductor crystals with semi-relativistic corrections in collaboration with Louie at California, Berkeley. Ishii implemented one-shot GW [12–17], Morisato (now Accerlys K.K.) improved accuracy of calculation and performed several calculations including core states, Farajian performed first-principles MD simulations of alkaline atom insertion to nanotube [18], Shiga performed calculations of transition metal clusters. TDDFT electron excited states dynamics simulations were first performed at IMR by Wu (now Tsinghua Univ., Beijing), and later at YNU by Sawada and Kodama [19–25]. Then, at YNU, Furuya, Noguchi (now Inst. Solid State Phys. (ISSP), Univ. of Tokyo), Nagaoka performed dielectric functions of TTTA crystal and CdSe clusters [26], and Iwata performed GW calculations of semiconductor crystals [27].

Simultaneously, at IMR, Sluiter (now Delft Univ. of Tech.) completely rewrite the LDA part of the program with Fortran90 and parallelized with hybrid MPI and OpenMP, and completed Ver. 1 of TOhoku Mixed Basis Orbital (TOMBO). [28–30]. Adachi (Hitachi Solutions East Japan, Ltd.), Sahara (now Nat. Inst. Mater. Sci. (NIMS)) tried to include GGA and extend it to be applicable to crystals. Bae performed calculations of transition metal clusters [32–34], Nishimatsu calculate XPS spectra of Si crystal [35], and Bahramy et al. successfully applied this program to hyperfine constants [36]. More recently, Sluiter and Sahara developed Ver. 2 of TOMBO, which can perform TDDFT dynamics simulations with semi-relativistic corrections. Some of these results were summarized and reviewed by Kawazoe et al. in a book [37].

More recently, Noguchi parallelized the original code having LDA, LSDA, one-shot GW approximation, and Bethe–Salpeter equation [38–40] with MPI and openMP, and performed the calculation of the double ionization spectra by using the T -matrix method [41–46], the on-site Coulomb energy U of molecular Mott insulator [47], the Moller Plesset 2nd order calculation, Auger spectra [48], and photoabsorption spectra [49, 50]. In YNU, Tadokoro implemented the Hartree-Fock calculation, and Kuwahara implemented the self-consistent GW calculation (with and without vertex correction) in TOMBO.

What we explain below is the detailed algorithms used in this purely original all-

electron mixed basis program TOMBO. It uses numerical atomic orbitals (AOs) in addition to plane waves (PWs). This approach can describe both spatially localized to extended orbitals. TOMBO can calculate the electronic states from isolated clusters to periodic crystals with relatively small number of basis functions.

2 Survey of All-Electron Mixed Basis Approach

2.1 DFT and LDA

Under density functional theory (DFT)[1], it is formally possible to write the total energy E of arbitrary systems composed of electrons and nuclei as a sum of a universal functional $F[\rho(\mathbf{r})]$ of only the total electron charge density distribution $\rho(\mathbf{r})$ and the external energy $E_{ext}[\rho(\mathbf{r})] = \int v(\mathbf{r})\rho(\mathbf{r})d\mathbf{r}$ due to the external potential $v(\mathbf{r})$, which is the Coulomb potential caused by the nuclear point charges and independent of $\rho(\mathbf{r})$. If we subtract from $F[\rho(\mathbf{r})]$ the classical electrostatic energy between electrons, which is called the Hartree energy and is simply given by

$$E_H[\rho(\mathbf{r})] = \frac{e^2}{4\pi\epsilon_0} \int d\mathbf{r}d\mathbf{r}' \frac{\rho(\mathbf{r})\rho(\mathbf{r}')}{|\mathbf{r} - \mathbf{r}'|}, \quad (1)$$

the rest is called the exchange-correlation energy $E_{xc}[\rho(\mathbf{r})]$, which expresses the exchange and correlation parts of the electron total energy. Therefore total energy E is composed of three parts, the Hartree energy, the exchange-correlation energy, and the external energy, as follows: $E[\rho(\mathbf{r})] = E_H[\rho(\mathbf{r})] + E_{xc}[\rho(\mathbf{r})] + E_{ext}[\rho(\mathbf{r})]$. The important point is that this total energy $E[\rho(\mathbf{r})]$ of the system is a universal functional of only $\rho(\mathbf{r})$, and $E[\rho(\mathbf{r})]$ has a minimum value when ρ is the true electron charge density distribution at the electronic ground state. This last statement comes from the variational principle in standard quantum mechanics.

It is natural to write the electron charge density distribution $\rho(\mathbf{r})$ as a sum of the absolute square of effective one-electron wave functions over all occupied states:

$$\rho(\mathbf{r}) = \sum_{\nu} |\phi_{\nu}(\mathbf{r})|^2. \quad (2)$$

These effective one-electron wave functions should be normalized as

$$\int |\phi_{\nu}(\mathbf{r})|^2 d\mathbf{r} = 1. \quad (3)$$

Then, the kinetic energy can be at least approximately written as

$$T_s[\rho(\mathbf{r})] = -\frac{\hbar^2}{2m} \sum_{\nu} \int \phi_{\nu}^*(\mathbf{r}) \nabla^2 \phi_{\nu}(\mathbf{r}) d\mathbf{r}. \quad (4)$$

Now, by taking the functional derivative of the total energy $E[\rho(\mathbf{r})]$ with respect to the complex conjugate of the effective one-electron wave function, $\phi_\nu^*(\mathbf{r})$, under the constraint of the norm conservation (3), we will have

$$\left(-\frac{\hbar^2}{2m}\nabla^2 + V_H[\rho(\mathbf{r})] + V_{xc}[\rho(\mathbf{r})] + V_{ext}\right)\phi_\nu(\mathbf{r}) = \varepsilon_\nu\phi_\nu(\mathbf{r}). \quad (5)$$

Here ε_ν is the Lagrange multiplier introduced by guaranteeing the norm conservation. The second and third terms inside the bracket in the l.h.s. are the Hartree potential given by

$$V_H[\rho(\mathbf{r})] = \frac{e^2}{4\pi\varepsilon_0} \int \frac{\rho(\mathbf{r}')}{|\mathbf{r} - \mathbf{r}'|} d\mathbf{r}', \quad (6)$$

and the exchange-correlation potential $V_{ext}[\rho(\mathbf{r}')]$ defined as a functional derivative with respect to $\rho(\mathbf{r}')$ as

$$V_{ext}[\rho(\mathbf{r}')] = \frac{\delta E_{ext}[\rho(\mathbf{r})]}{\delta\rho(\mathbf{r}')} . \quad (7)$$

The problem here is that we do not know the form of $V_{ext}[\rho(\mathbf{r}')]$. Equation (5) is called the Kohn–Sham equation and its solution $\phi_\nu(\mathbf{r})$ is called the Kohn–Sham wave function.

In a homogeneous electron gas system, where the nuclear point charges are replaced by a homogeneous positive background charge, the electron charge density $\rho(\mathbf{r})$ becomes just a constant ρ everywhere, so that the universal functional $F[\rho(\rho)]$ of the spatial function $\rho(\mathbf{r})$ becomes just a function $F(\rho)$ of a value ρ . Using a very accurate quantum Monte Carlo simulation [53], one may precisely determine the total energy of the electron gas system at the ground state as a function of the homogeneous electron density ρ , which is the negative of the homogeneous positive background charge density due to the charge neutrality of the whole system. That is, we know the explicit form of the function $F(\rho)$ in the homogeneous electron gas system. If we subtract the classical electrostatic energy between electrons (the Hartree energy) from this $F(\rho)$, we identify the exchange-correlation energy $E_{xc}(\rho)$. Then the exchange-correlation potential $V_{xc}(\rho)$ is given by a simple derivative of $E_{xc}(\rho)$ with respect to ρ .

Within the local density approximation (LDA)[2], the last exchange-correlation potential $V_{xc}(\mathbf{r})$ at point \mathbf{r} becomes simply a universal function (not a functional) of the total electron charge density $\rho = \rho(\mathbf{r})$ at point \mathbf{r} . In this approximation, it is readily known that $V_{xc}(\mathbf{r}) = V_{xc}(\rho)$ is given by the exchange-correlation potential of the electron gas system having the same electron density ρ everywhere in the system. There are several interpolation formulae proposed so far. In TOMOB, Perdew–Zunger’s formula[52] is used as a default setting.

Therefore, once the total electron density distribution $\rho(\mathbf{r})$ at point \mathbf{r} is known, the exchange-correlation potential at this point can be determined uniquely. This is a very

simple idea, which makes all the calculation scheme very tractable. Using this LDA, we can solve this Kohn–Sham equation self-consistently.

2.2 Atomic Orbitals and Non-Overlapping Spheres

For an isolated atom, it is possible to solve the Kohn–Sham equation very rigorously, because of the system has a spherical symmetry. In this case, the Kohn–Sham wave function is expressed as a product of radial function $R_{jnl}(r)$ and spherical harmonics $Y_{lm}(\hat{\mathbf{r}})$ as

$$\phi_{jnml}^{\text{AO}}(\mathbf{r}) = Y_{lm}(\hat{\mathbf{r}})R_{jnl}(r). \quad (8)$$

Here, j , n , l , and m are atomic species, principal quantum number, angular momentum quantum number, and magnetic quantum number. (TOMBO uses cubic harmonics instead of spherical harmonics, and all integrals involving cubic harmonics are performed analytically.) We can solve numerically the one-dimensional differential equation in radial direction for $R_{jnl}(r)$. The atomic orbitals (AOs) used in our mixed basis code are generated in this way. We use the Herman–Skillman code [51] modified to use logarithmic radial mesh by Akira Hasegawa. The number of mesh is set at 621 in TOMBO. The radial function $R_{jnl}(r)$ is defined as B or Bs in the code. Bs is the function having the same radial factors $\sqrt{4\pi}$ (S-orbital), $r\sqrt{4\pi}/\sqrt{3}$ (P-orbital), $r^2\sqrt{4\pi}/\sqrt{15}$ (D-orbital), $r^3\sqrt{4\pi}/\sqrt{105}$ (F-orbital) as in the Herman–Skillman code, while B is defined without these factors to use the ordinary normalization in the xyz coordinates.

Although the core AOs are usually well localized and have no overlap with different AOs centered at adjacent atoms. For the valence AOs, however, they overlap with neighboring atoms. In order to restrict them inside the non-overlapping atomic sphere of cutoff radius (rct), we subtract from the original AO a smooth function (a simple polynomial function) which satisfies matching condition, i.e., which has the same value and the same derivative at rct (Fig.1). This smooth function inside the atomic sphere smoothly connects to the original AO outside the atomic sphere. Thus, this overall smooth function can be well described by PWs. This technique has two merits: One is that we can avoid complicated calculation of overlap integrals between different atoms, and the other is that we can reduce the overcompleteness problem, because the subtracted AOs are more localized than the original AOs.

2.3 Mixed Basis Formulation

In the mixed basis code, the Kohn–Sham wave function is expressed as a linear combination of plane waves (PWs) and atomic orbitals (AOs) as follows:

$$\psi_{\nu}(\mathbf{r}) = \frac{1}{\sqrt{\Omega}} \sum_{\mathbf{G}} c_{\nu}^{\text{PW}}(\mathbf{G})e^{i\mathbf{G}\cdot\mathbf{r}} + \sum_j \sum_{nlm} c_{\nu}^{\text{AO}}(jnml)\phi_{jnml}^{\text{AO}}(\mathbf{r} - \mathbf{R}_j) \equiv \sum_{\xi} c_{\nu,\xi} f_{\xi}(\mathbf{r}) \quad (9)$$

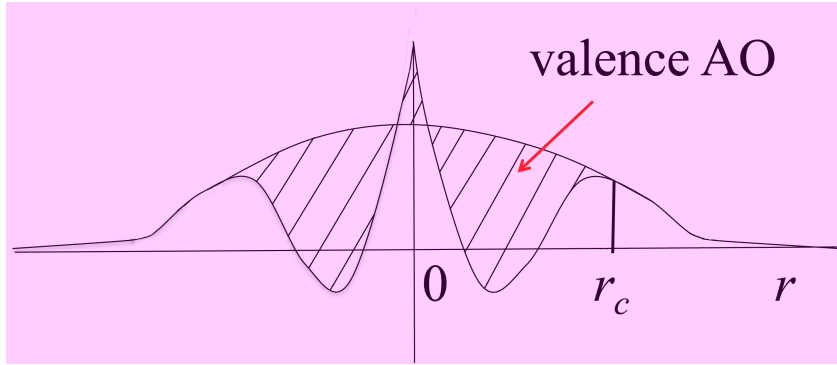


Fig. 1: Subtraction of valence atomic orbitals (AOs). By subtracting a simple polynomial smooth function having the same value and the same derivative at the radius r_c , we can define new AOs that has finite values only inside the atomic sphere. This polynomial connects smoothly to the original AO, and can be expressed by a linear combination of PWs.

Here Ω is the volume of the unit cell (om in the code), c is the expansion coefficients (cr,ci,dr9,di9,... in the code), $\phi_{nlm}^{\text{AO}}(\mathbf{r})$ is the AOs defined in (8).

We divide the total electron charge density distribution $\rho(\mathbf{r})$ into two parts: one is the spherically symmetric part (ro, roT) defined inside each non-overlapping atomic sphere, and the rest is the global part defined in the whole unit cell. The first one is mainly made of AOs and has only nonzero values inside the non-overlapping atomic spheres. The effective potential is also divided in a similar way (Fig.2). Thus it becomes possible

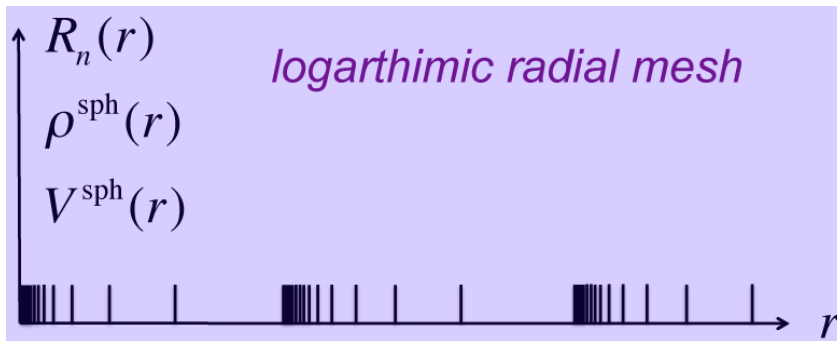


Fig. 2: Radial function $R_{nl}(r)$ of an atomic orbital (AO), the spherically symmetric charge density $\rho^{\text{sph}}(r)$, and the spherically symmetric effective potential $V^{\text{sph}}(r)$ defined inside non-overlapping atomid sphere.

to perform very accurate calculations both for isolated systems and periodic systems in the same way.

The semi-relativistic correction (Darwin and mass-velocity terms) can be included in

the calculation if the input parameter `irelativistic = 1` is set in `INPUT.inp`.

Since the basis functions $f_{\xi}(\mathbf{r})$ are not orthogonal each other, the eigenvalue ε_{ν} is obtained by solving the following generalized eigenvalue problem:

$$\sum_{\xi'} H_{\xi\xi'} c_{\nu,\xi'} = \varepsilon_{\nu} \sum_{\xi'} S_{\xi\xi'} c_{\nu,\xi'}, \quad (10)$$

where $H_{\xi\xi'} = \langle f_{\xi} | H | f_{\xi'} \rangle$ and $S_{\xi\xi'} = \langle f_{\xi} | f_{\xi'} \rangle$ are, respectively, the Hamiltonian and overlap matrix elements between the ξ 'th and ξ' 'th basis functions. Here, if we introduce the column vector

$$\Psi_{\nu} \equiv \begin{pmatrix} c_{\nu,1} \\ c_{\nu,2} \\ \vdots \\ c_{\nu,\xi} \\ \vdots \\ c_{\nu,N_{\text{bs}}} \end{pmatrix}, \quad (11)$$

(N_{bs} is the number of basis functions (nbs in the code)), Eq.(10) can be rewritten as follows:

$$H\Psi_{\nu} = \varepsilon_{\nu} S\Psi_{\nu}. \quad (12)$$

This generalized eigenvalue problem is transformed to the usual eigenvalue problem by using Choleski decomposition. The overlap matrix S is expressed as a product of a lower triangular matrix T and its Hermitian conjugate T^{\dagger} :

$$S = TT^{\dagger}. \quad (13)$$

Then, Eq. (12) becomes

$$H'\Phi_{\nu} = \varepsilon_{\nu}\Phi_{\nu}, \quad (14)$$

with the transformed Hamiltonian

$$H' = T^{-1}HT^{\dagger^{-1}}, \quad (15)$$

(H' is calculated from H and T^{-1}), and the transformed eigenvectors are give by

$$\Phi_{\nu} = T^{\dagger}\Psi_{\nu}. \quad (16)$$

The resulting ordinary eigenvalue problem can be solved by the standard library program using the Hausholder method, or the steepest-descent method as

$$\Phi_{\nu}(t + \Delta t) = \Phi_{\nu}(t) - (T^{-1}H(t)\Psi_{\nu}(t) - \varepsilon_{\nu}(t)\Phi_{\nu}(t))\mu^{-1}\Delta t + \sum_{\mu} \Lambda_{\nu\xi}\Phi_{\xi}(t + \Delta t), \quad (17)$$

$$\varepsilon_{\nu}(t) = \Phi_{\nu}^{\dagger}(t)T^{-1}H(t)\Psi_{\nu}(t), \quad (18)$$

where the matrix Λ is the Lagrange multiplier, and determined so as to orthogonalize the eigenvectors $\Psi_\nu(t + \Delta t), (\nu = 1, 2, \dots)$. However, instead of determining Lagrange multiplier, standard Gram–Schmidt orthogonalization is used in the code. In Eq.(17), parameter μ describes the difficulty of changing the electronic states toward the self-consistent solution. If we adopt the SD method (18), it is not necessary to evaluate H' given in (15). Here, all the quantities $H, \varepsilon_\nu, \Psi_\nu,$ and ϕ_ν depend on the fictitious time step t . The Hamiltonian at (fictitious) time $t + \Delta t$ is determined by the total charge density at the time, which was constructed by using the state vector at time t . Figure3 describes the flowchart of this algorithm. The global subroutine names called from the main program (mdmain.f) are written in the right hand side.

In the program, the total number of atomic orbitals is nao, the maximum number of the number of atomic orbitals of different atomic species is kao. The maximum number of the integer indices of reciprocal lattice vectors \mathbf{G} for PWs is nod, and the corresponding number of PWs is nw. nw is set automatically by setting nod or Ecutoff, which is the cutoff energy of PWs, corresponding the maximum kinetic energy of PWs.

As the other important parameters used in the code, noc is the number of occupied states, nol is the number of levels (states), and nStep is the number of steps in the MD simulation, iSblp is the maximum number of self-consistent field (SCF) iterations, and smixSCF is the mixing rate of the previous charge density in the SCF loop. dTime is the time step in units of femto second (fs). dteq is the fictitious time used in the Steepest-Descent method $\Delta t/\mu$.

2.4 All-Electron Charge Density and Potential

In the all-electron mixed basis approach, all-electron charge density $\rho(\mathbf{r})$ is made of three contributions: PW-PW, AO-PW, and AO-AO.

$$\rho(\mathbf{r}) = \rho^{\text{PW-PW}}(\mathbf{r}) + \sum_j \rho_j^{\text{AO-PW}}(\mathbf{r}) + \sum_j \rho_j^{\text{AO-AO}}(\mathbf{r}) \quad (19)$$

These contributions are given, respectively, as

$$\rho^{\text{PW-PW}}(\mathbf{r}) = \frac{2}{\Omega} \sum_\nu^{\text{occ}} \sum_{\mathbf{G}} \sum_{\mathbf{G}'} c_\nu^{\text{PW}*}(\mathbf{G}') c_\nu^{\text{PW}}(\mathbf{G}) e^{i(\mathbf{G}-\mathbf{G}')\cdot\mathbf{r}},$$

$$\rho_j^{\text{AO-PW}}(\mathbf{r}) = \frac{2}{\sqrt{\Omega}} \sum_\nu^{\text{occ}} \sum_{nlm} c_\nu^{\text{AO}*}(jnlm) c_\nu^{\text{PW}}(\mathbf{G}) \phi_{jnlm}(\mathbf{r} - \mathbf{R}_j) e^{i\mathbf{G}\cdot\mathbf{r}} + \text{c.c.}, \quad (20)$$

$$\rho_j^{\text{AO-AO}}(\mathbf{r}) = 2 \sum_\nu^{\text{occ}} \sum_{n'l'm'} c_\nu^{\text{AO}*}(jn'l'm') c_\nu^{\text{AO}}(jnlm), \phi_{jn'l'm'}(\mathbf{r} - \mathbf{R}_j) \phi_{jnlm}(\mathbf{r} - \mathbf{R}_j). \quad (21)$$

Here the prefactor 2 denotes the spin duplicity, and \sum_ν^{occ} means the sum over all occupied states. The first PW-PW contribution can be conveniently treated in Fourier space. The

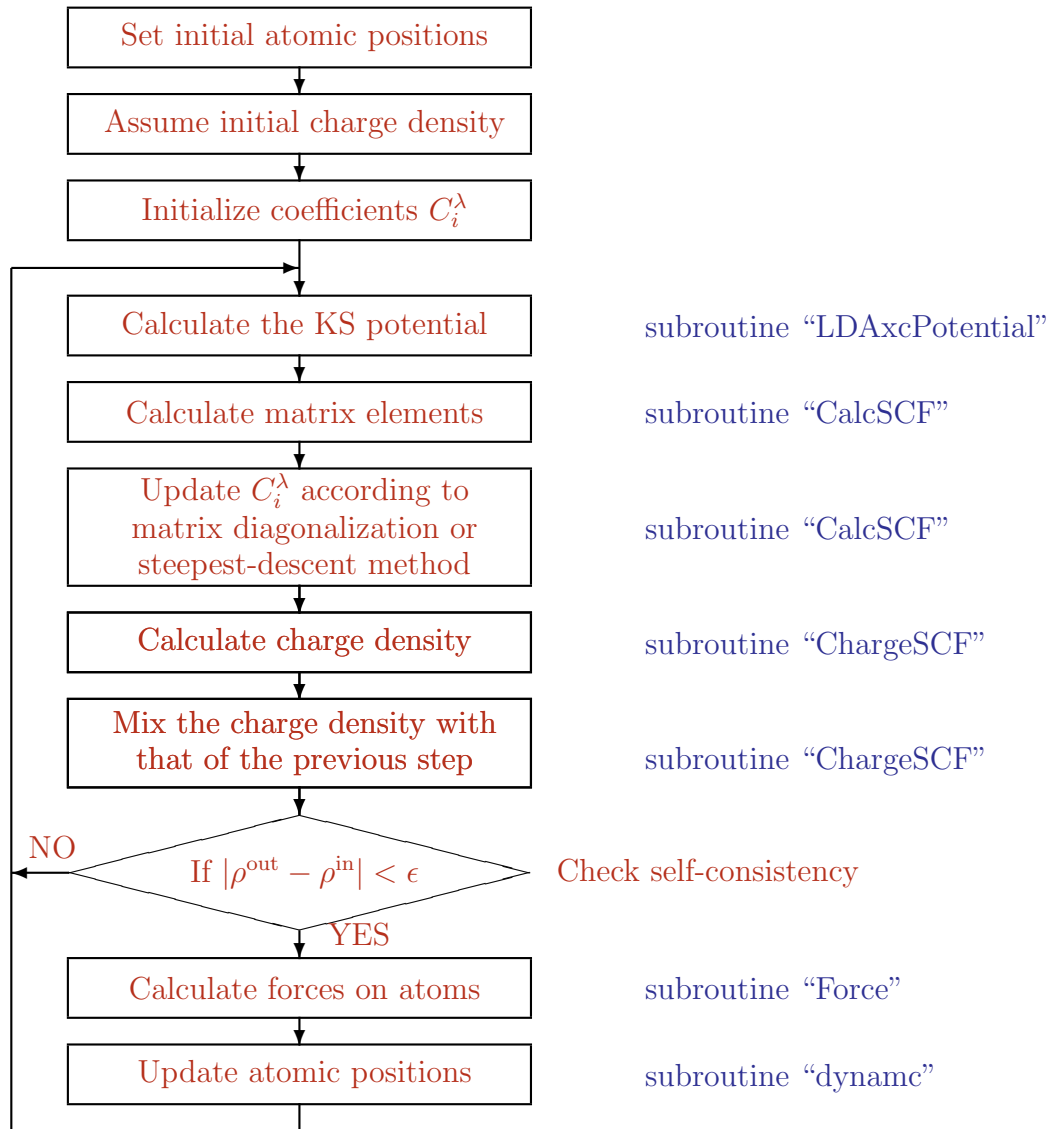


Fig. 3: Flowchart of the first-principles molecular dynamics using matrix diagonalization, steepest-descent (SD), or conjugate-gradient (CG) methods (global subroutine names are written in the right hand side). The convergence of the electronic states is checked by the difference of the total energy between the present and previous iteration steps. If convergence is achieved, the atomic positions are updated by using the calculated force.

rest two AO-related contributions are confined only inside the non-overlapping atomic spheres, and can be written together as

$$\rho_j^{\text{AO}}(\mathbf{r}) = \rho_j^{\text{AO-PW}}(\mathbf{r}) + \rho_j^{\text{AO-AO}}(\mathbf{r}). \quad (22)$$

This can be divided into two parts: one is spherical symmetric part and the other is asymmetric part. The former is written as the sum of $\sigma_j(|\mathbf{r} - \mathbf{R}_j|)$, which is the spherical average of $\rho_j^{\text{AO}}(\mathbf{r})$ given by

$$\sigma_j(|\mathbf{r} - \mathbf{R}_j|) = \frac{1}{4\pi} \int \rho_j^{\text{AO}}(\mathbf{r}) d\Omega_j, \quad (23)$$

where Ω_j is the solid angle around the j th atom. Each $\sigma_j(r)$ is stored as a 1D function of radius r (ro, roT in the code) similar to the radial function $R_{jnl}(r)$ of AOs. The other asymmetric term $\rho_j^{\text{asym}}(\mathbf{r})$ is given by subtracting this symmetric part $\sigma_j(|\mathbf{r} - \mathbf{R}_j|)$ from the total AO-related charge density $\rho_j^{\text{AO}}(\mathbf{r})$:

$$\rho_j^{\text{asym}}(\mathbf{r}) = \rho_j^{\text{AO}}(\mathbf{r}) - \sigma_j(|\mathbf{r} - \mathbf{R}_j|). \quad (24)$$

This part is added to $\rho^{\text{PW-PW}}(\mathbf{r})$ and treated as $\rho^{\text{rest}}(\mathbf{r})$.

$$\rho^{\text{rest}}(\mathbf{r}) = \rho^{\text{PW-PW}}(\mathbf{r}) + \sum_j \rho_j^{\text{asym}}(\mathbf{r}). \quad (25)$$

These AO-related charge densities are calculated in the subroutine radial_Charge (iAsym=0) or radial_Charge2 (iAsym=1). The asymmetric part is generally negligible, but if necessary can be taken into account by setting the option parameter iAsym = 1 in INPUT.inp.

Thus the total charge density is written as

$$\rho(\mathbf{r}) = \rho^{\text{rest}}(\mathbf{r}) + \sum_j \sigma_j(|\mathbf{r} - \mathbf{R}_j|), \quad (26)$$

where $\rho^{\text{rest}}(\mathbf{r})$ is the same as $\rho^{\text{PW-PW}}(\mathbf{r})$ when iAsym = 0.

The treatment of ignoring asymmetric part of the AO-related charge density is guaranteed as a good approximation, and usually iAsym is set zero. First of all, this approximation keeps the total charge neutrality because the integrated value of the asymmetric part is zero. Next, since $\sigma_j(r)$ is restricted inside non-overlapping atomic spheres, the asymmetric part in this region is expected to be very small. However, for example, when one wants to treat core states accurately, one has to treat the asymmetric part as well.

To treat asymmetric part with enough accuracy, it is required to set large enough “nog” (for example nog = 30) in INPUT.inp and increase the number of mesh (“mesh”) discretizing the unit cell. This can be done by setting, for example, mesh = 128 in COORDINATES.inp. (Note that the parameter “nog”, which is usually used in GW or Hartree-Fock calculation, is also used for the treatment of the asymmetric AO-related

charge density.) The discretized unit cell by mesh \times mesh \times mesh is called the global mesh space in contrast to the spherically symmetric space inside the non-overlapping atomic sphere. The global mesh space can be often Fourier transformed to the reciprocal lattice space by using the fast Fourier transformation (FFT). The total charge density defined by Eq.(19) or Eq.(26) is calculated in either in reciprocal lattice space or inside the non-overlapping atomic sphere in logarithmic radial mesh.

One the total electron density is evaluated in the global mesh space and in the radial mesh inside atomic sphere, the exchange-correlation potential in LDA can be calculated. That is, the exchange-correlation potential in the global mesh space $\mu^{\text{xc}}(\mathbf{r})$ and its spherically symmetric part on the radial mesh inside atomic sphere are obtained straightforwardly. The latter spherically symmetric part is then truncated inside the non-overlapping atomic sphere to form a confined function, which goes smoothly to zero at the radius of atomic sphere, r_{ct} . It is stored as the truncated spherical exchange-correlation potential, $\mu_j^{\text{xc}}(|\mathbf{r} - \mathbf{R}_j|)$. (This truncation is done by subtracting smooth quadratic function satisfying the matching condition at r_{ct} in a similar way to that used to confine AOs inside r_{ct} described in Fig.1.) On the other hand, the former global mesh part $\mu^{\text{xc}}(\mathbf{r})$ is subtracted by this truncated spherical part $\mu_j^{\text{xc}}(|\mathbf{r} - \mathbf{R}_j|)$. The resulting “rest part”

$$\mu^{\text{xc rest}}(\mathbf{r}) = \mu^{\text{xc}}(\mathbf{r}) - \sum_j \mu_j^{\text{xc}}(|\mathbf{r} - \mathbf{R}_j|). \quad (27)$$

is a smooth function without cuspidal behavior in the global mesh space. Obviously, the total exchange-correlation potential is given by the sum of the truncated spherical part and the rest global part. The important point in this procedure is that the rest global part is smooth enough and can be easily Fourier transformed into the reciprocal lattice space by using the FFT. This Fourier transformed rest part $\bar{\mu}^{\text{xc}}(\mathbf{G})$ together with the 1D Fourier transformation of the truncated spherical part in radial direction $\bar{\mu}^{\text{xc rest}}(\mathbf{G})$ gives the total exchange-correlation potential in the reciprocal lattice space, which is used as the exchange-correlation part of the PW-PW potential matrix elements.

In this way, the potential matrix elements sandwiched by PWs is equal to the Fourier coefficients of the total potential $V(\mathbf{r})$. So we need to calculate other contributions to the total potential. Fourier coefficients of the Coulomb potential from nucleus charge $\bar{V}^{\text{nuc}}(\mathbf{G})$ is given by

$$\bar{V}^{\text{nuc}} = -\frac{4\pi}{\Omega} \sum_j e^{i\mathbf{G}\cdot\mathbf{R}_j} \frac{Z_j}{G^2}. \quad (28)$$

Fourier coefficients of the Hartree potential $\bar{V}^{\text{H}}(\mathbf{G})$ can be readily calculated by using $\bar{\rho}(\mathbf{G})$ as

$$\bar{V}^{\text{H}}(\mathbf{G}) = 4\pi \frac{\bar{\rho}(\mathbf{G})}{G^2}. \quad (29)$$

The way of determining Fourier coefficients of the exchange-correlation potential $\bar{\mu}^{\text{xc}}(\mathbf{G})$ was described above. Thus the Fourier coefficients of the total potential $\bar{V}(\mathbf{G})$ is expressed as a sum of the three terms: $\bar{V}^{\text{nuc}}(\mathbf{G})$, $\bar{V}^{\text{H}}(\mathbf{G})$, and $\bar{\mu}^{\text{xc}}(\mathbf{G})$.

2.5 AO-Related Matrix Elements

On the other hand, we need to evaluate the AO-related matrix elements (PW-AO & AO-AO). We have to provide potential $V(\mathbf{r})$ inside atomic spheres separately for these matrix elements. This is because AOs are strongly localized and it is extremely difficult to express its potential in the global mesh space. Here, we assume that the potential $V(\mathbf{r})$ used for the AO-related matrix elements is spherical symmetric inside non-overlapping atomic spheres. It is, however, possible to introduce asymmetric potential inside the non-overlapping atomic spheres by setting `iAsym = 1`. Then the asymmetric contribution to the AO-related matrix elements is evaluated by using 1D Fourier transformations in radial direction. However, the result becomes accurate only when one uses enough large `nog` and `mesh`.

In usual case, again one can ignore this asymmetric contribution, because it is expected that all AOs have relatively large amplitudes in the core region where the self-consistent potential is almost spherically symmetric. Note that this approximation is completely different from the idea of the muffin-tin approximation, because, in our case, the asymmetric part still exists in the potential for PWs, which spans the whole unit cell even inside the non-overlapping atomic spheres.

Hereafter, let us consider spherical potential around each nucleus $V_j(r_j)$. Here we put $r_j = |\mathbf{r} - \mathbf{R}_j|$. First, consider the Hartree potential made by the AO-related spherically symmetric charge $\sigma_j(r_j)$ centered at \mathbf{R}_j . This potential is easily calculated as the 1D integration in radial direction of the Poisson equation as follows:

$$v_j^{\text{H}}(r_j) = \frac{4\pi}{r_j} \int_0^{r_j} \sigma_j(r) r^2 dr + 4\pi \int_{r_j}^{r_c} \sigma_j(r) r dr. \quad (30)$$

According to the Gauss theorem in electrostatics, this Hartree potential behaves as

$$v_j^{\text{H}}(r_j) = \frac{Q_j}{r_j}, \quad \text{for } r \geq r_c, \quad (31)$$

where Q_j is the symmetric charge defined as

$$Q_j = 4\pi \int_0^{r_c} \sigma_j(r) r^2 dr. \quad (32)$$

On the other hand, if we define the screened charge Z_j^* as

$$Z_j^* = Z_j - Q_j, \quad (33)$$

(Z_j is atomic number), the sum of the Hartree potential $v_j^{\text{H}}(r_j)$ and nuclear Coulomb potential $-Z_j/r_j$ around \mathbf{R}_j becomes

$$v_j^{\text{H}}(r_j) - \frac{Z_j}{r_j} = -\frac{Z_j^*}{r_j}, \quad \text{for } r_j \geq r_c \quad (34)$$

outside the non-overlapping atomic sphere. Because of this long tail, it is necessary to add all the contributions from surrounding atoms. This summation should be taken not only inside the own unit cell, but also surrounding or further apart unit cells. To treat this accurately, we use the following Fourier decoupling method. In this method, the simple potential form $-Z_j^*/r_j$ given by Eq.(34) connects smoothly to the quadratic function inside the non-overlapping atomic sphere. They should have the same value and the same derivative at the radius of the atomic sphere $r = r_c$:

$$v_j^{\text{interpo}}(r_j) = \begin{cases} Z_j^*(br_j^2 + d) & \text{for } r_j < r_c, \\ -Z_j^*/r_j & \text{for } r_j \geq r_c. \end{cases} \quad (35)$$

From the matching condition, we obtain

$$\begin{aligned} br_c^2 + d &= -1/r_c, \\ 2br_c &= 1/r_c^2. \end{aligned} \quad (36)$$

From simple calculation, we find that these conditions are identical to

$$b = \frac{1}{2r_c^3}, \quad d = -\frac{3}{2r_c}. \quad (37)$$

Thus connected potential is a smooth and analytic function over whole space and is easily transformed into reciprocal lattice space analytically. We call this potential the interpolated Coulomb potential and write it as $v_j^{\text{interpo}}(r_j)$; see Eq.(35). This interpolated Coulomb potential takes the correct value of the Coulomb potential, $v_j^{\text{H}}(r_j) - \frac{Z_j}{r_j}$, everywhere outside the j th atomic sphere; It takes an incorrect value only inside the j th atomic sphere, and its difference from the correct value is given by

$$V_j^{\text{trunc}}(r_j) = v_j^{\text{H}}(r_j) - \frac{Z_j}{r_j} - v_j^{\text{interpo}}(r_j), \quad (38)$$

which we call the truncated Coulomb potential. It has nonzero values only each atomic sphere, and is spherically symmetric. This truncation is schematically illustrated in Fig.4. This truncated Coulomb potential is added to the truncated spherical exchange-correlation potential $\mu_j^{\text{xc}}(|\mathbf{r} - \mathbf{R}_j|)$ and stored as one-dimensional data on the radial logarithmic mesh.

Apart from this truncated function, we have to treat separately interpolated Coulomb potential $v_j^{\text{interpo}}(r_j)$. This function $v_j^{\text{interpo}}(r_j)$ is analytically expressed by Eq.(35) in

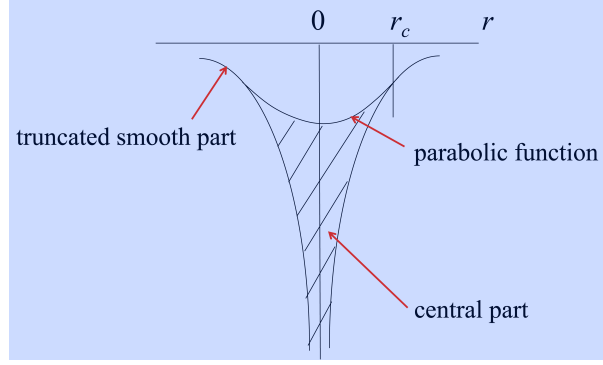


Fig. 4: Truncation of AO-screened nuclear Coulomb potential using the interpolation in terms of quadratic function.

infinite space, and therefore is able to be analytically transformed into \mathbf{G} space. The Fourier coefficients are explicitly given by

$$\bar{v}_j^{\text{interpo}}(\mathbf{G}) = \frac{4\pi Z_j e^{-i\mathbf{G}\cdot\mathbf{R}_j}}{\Omega} \left\{ b \left[\left(3(Gr_c)^2 - 6 \right) \sin Gr_c + 6Gr_c \cos Gr_c \right] / G^5 + d \sin Gr_c / G^3 + \cos Gr_c / G^2 \right\}. \quad (39)$$

This analytic Fourier coefficients are added to the rest part of the Fourier coefficients of both the Hartree potential $\bar{\rho}^{\text{rest}}(\mathbf{G})$ and the exchange-correlation potential $\bar{\mu}^{\text{xc rest}}(\mathbf{G})$ to give an additional contribution to the spherical potential in the j th atomic sphere. That is, this additional contribution to the spherical potential from the three kinds of Fourier coefficients are expressed as:

$$V_j^{\text{rest}}(r_j) = \sum_{\mathbf{G}} \frac{\sin Gr_j}{Gr_j} e^{i\mathbf{G}\cdot\mathbf{R}_j} \left[\sum_k \bar{V}_k^{\text{interpo}}(\mathbf{G}) + \frac{4\pi \bar{\rho}^{\text{rest}}(\mathbf{G})}{\Omega G^2} + \bar{\mu}^{\text{xc rest}}(\mathbf{G}) \right]. \quad (40)$$

Here we note that $v_j^{\text{interpo}}(r_j)$ defined by Eq.(35) is different from the first term in the l.h.d. of Eq.(40). The latter includes all the tails of the interpolated Coulomb potential centered at all $k \neq j$ atoms. This is obvious from the nature of the Fourier transformation.

Thus the total effective potential to be used in the AO-related matrix elements are given by

$$V_j(r_j) = V_j^{\text{trunc}}(r_j) + V_j^{\text{rest}}(r_j). \quad (41)$$

All the AO-related matrix elements are calculated by using this spherical potential. The contribution from the asymmetric part of the potential is treated separately in a large Fourier space when `iAsym = 1` is set in `INPUT.inp`.

2.6 Total Energy and Force

Total energy and force are calculated as follows. First, total energy is given by $E^{\text{tot}} = E^{\text{el}} + E^{\text{ii}}$, where E^{el} denotes the electron part and E^{ii} denotes the Coulomb energy between nuclei. The former E^{el} is the sum of the electron kinetic energy K and potential energy W , which is given by

$$W = \frac{1}{2} \int \frac{\rho(\mathbf{r})\rho(\mathbf{r}')}{|\mathbf{r} - \mathbf{r}'|} d\mathbf{r}d\mathbf{r}' - \sum_j Z_j \int \frac{\rho(\mathbf{r})}{|\mathbf{r} - \mathbf{R}_j|} d\mathbf{r} + E^{\text{xc}}. \quad (42)$$

Here, E^{xc} is the exchange-correlation energy. The latter E^{ii} is given by

$$E^{\text{ii}} = \frac{1}{2} \sum_{k \neq j} \frac{Z_j Z_k}{|\mathbf{R}_j - \mathbf{R}_k|}, \quad (43)$$

which is evaluated by the Ewald sum. The total energy is calculated more conveniently with the expression

$$E^{\text{total}} = 2 \sum_{\nu} \varepsilon_{\nu} - \frac{1}{2} \int \frac{\rho(\mathbf{r})\rho(\mathbf{r}')}{|\mathbf{r} - \mathbf{r}'|} d\mathbf{r}d\mathbf{r}' + E^{\text{xc}} - \int \rho(\mathbf{r})\mu^{\text{xc}}(\mathbf{r})d\mathbf{r}. \quad (44)$$

Next, force is calculated as follows. Here we briefly describe the points where we have particularly elaborated in the force calculation. Since AOs do not penetrate into adjacent atomic spheres, we can use Gauss theorem several times to obtain

$$\begin{aligned} \nabla_j E^{\text{tot}} &= \nabla_j \sum_{k(\neq j)} \frac{Z_j^* Z_k^*}{|\mathbf{R}_j - \mathbf{R}_k|} - Z_j \nabla_j \int \frac{\rho^{\text{PW-PW}}(\mathbf{r})}{|\mathbf{r} - \mathbf{R}_j|} d\mathbf{r} \\ &+ \int \frac{\rho^{\text{PW-PW}}(\mathbf{r}) \nabla_j \rho_j^{\text{AO}}(\mathbf{r}')}{|\mathbf{r} - \mathbf{r}'|} d\mathbf{r}d\mathbf{r}' + \int \rho_j^{\text{AO}}(\mathbf{r}) \nabla_j V_j(|\mathbf{r} - \mathbf{R}_j|) d\mathbf{r} \\ &+ \int \mu^{\text{xc}}(\mathbf{r}) \nabla_j \rho_j^{\text{AO}}(\mathbf{r}) d\mathbf{r} + \nabla_j K + \{(\nabla_j \Psi_{\nu}^{\dagger}) H \Psi_{\nu} + \text{c.c.}\}. \end{aligned} \quad (45)$$

The first and second terms in Eq.(45) are the same as the Hellmann–Feynman force appearing in the usual PW expansion. The first term is evaluated by the Ewald sum, and the second term is evaluated in Fourier space. The third to eighth terms are all so-called variational force, which occurs due to the dependence of AOs on the atomic positions. The third term and a part of the fourth term comes from the Hartree potential. The fourth term is similar to the external potential in the pseudopotential formalism. On the other hand, the derivative of E^{xc} with respect to \mathbf{R}_j (sixth term) is given by the fifth term of (45):

$$\begin{aligned} \nabla_j E^{\text{xc}} &= \int \frac{\delta E^{\text{xc}}}{\delta \rho(\mathbf{r})} \nabla_j \rho(\mathbf{r}) d\mathbf{r} = \int \mu^{\text{xc}}(\mathbf{r}) \nabla_j \rho_j^{\text{AO}}(\mathbf{r}) d\mathbf{r} \\ &\sim \int \mu^{\text{xc}}(\mathbf{r}) \nabla_j \sigma_j(|\mathbf{r} - \mathbf{R}_j|) d\mathbf{r} = i\Omega \sum_{\mathbf{G}} \mathbf{G} \bar{\mu}^{\text{xc}}(-\mathbf{G}) \bar{\sigma}_j(\mathbf{G}), \end{aligned} \quad (46)$$

where $\rho_j^{\text{AO}}(\mathbf{r})$ is approximated by its spherical symmetric form $\sigma_j(|\mathbf{r} - \mathbf{R}_j|)$ (this is done also in the third term). The seventh term is the derivative of the kinetic energy with respect to \mathbf{R}_j , in which only the cross term AO-K-PW contributes to the force. That is, we have

$$\nabla_j K = 2 \sum_{\nu}^{\text{occ}} \sum_{nlm} c_{\nu}^{\text{AO}*}(jnlm) c_{\nu}^{\text{PW}}(\mathbf{G}) \nabla_j \langle \phi_{jnlm} | K | \mathbf{G} \rangle + \text{c.c.}, \quad (47)$$

$$\nabla_j \langle \phi_{jnlm} | K | \mathbf{G} \rangle = \frac{\sqrt{\Omega}}{2} G^2 \bar{\phi}_{jnlm}(\mathbf{G}) \nabla_j \exp[i\mathbf{G} \cdot \mathbf{R}_j], \quad (48)$$

where $\bar{\phi}_{jnlm}(\mathbf{G})$ denotes the Fourier transform of the atomic orbital $\phi_{jnlm}(\mathbf{r})$. For a similar reason, also in the fourth term, the net contribution from ρ_j^{AO} appears only from the terms $\rho_j^{\text{AO-PW}}$. The last term, the eighth term, is the Pulay force representing the derivative of the coefficients in front of the basis functions with respect to \mathbf{R}_j . This term is evaluated as

$$\begin{aligned} & \{(\nabla_j \Psi_{\nu}^{\dagger}) H \Psi_{\nu} + \text{c.c.}\} = \varepsilon_{\nu} \{(\nabla_j \Psi_{\nu}^{\dagger}) \Psi_{\nu} + \text{c.c.}\} \\ & = \varepsilon_{\nu} \{ \nabla_j (\Psi_{\nu}^{\dagger} S \Psi_{\nu}) - \Psi_{\nu}^{\dagger} (\nabla_j S) \Psi_{\nu} \} = -\varepsilon_{\nu} \Psi_{\nu}^{\dagger} (\nabla_j S) \Psi_{\nu}. \end{aligned} \quad (49)$$

Here we use the identity $\Psi_{\nu}^{\dagger} S \Psi_{\nu} = 1$. In the last equality in Eq.(49), again, only the overlap integrals have nonzero contribution when either ($\xi \in \text{AO}$ and $\xi' \in \text{PW}$) or ($\xi \in \text{PW}$ and $\xi' \in \text{AO}$). This formulation about the derivative of the coefficients is the same as the formulation given by Ho et. al.[4,5] except for the pseudopotential formalism.

In TOMBO, first-principles molecular dynamics simulation can be performed by setting ‘‘M’’ in iApp in INPUT.inp. In this case, the number of dynamics steps, nStep, and dTime = Δt [fs] should be given also in INPUT.inp.

3 TDDFT Dynamics

According to the time-dependent density functional theory[54], TOMBO can treat the time-dependent Kohn–Sham (TDKS) equation

$$i \frac{\partial}{\partial t} \psi_j(\mathbf{r}, t) = H^q(\mathbf{r}, t) \psi_j(\mathbf{r}, t), \quad (50)$$

by setting ‘‘A’’ in iApp in INPUT.inp Here $H^q(\mathbf{r}, t)$ is the electronic part of the Hamiltonian. Combining this time-evolution equation with the Newtonian equation of motion for nuclei

$$M_A \ddot{\mathbf{R}}_A = - \frac{\partial}{\partial \mathbf{R}_A} [E^q + V^cl], \quad (51)$$

we can perform semi-classical dynamics simulation within the mean-field-type Ehrenfest theorem[55]. During one simulation, all dynamical variables change in time along one

reaction path according to the choice of the initial atomic coordinates and initial atomic velocities (velocities can be written parallel to the right of the coordinates in COORDINATES.inp). This way of simulation is called “on the fly” approach. Here E^q is the electronic part of the total energy, and, together with the Coulomb potential between nuclei V^{cl} , gives the mean-field potential exerting on nuclei. In these equations, \mathbf{r} is the electron coordinate, M_A and \mathbf{R}_A are the mass and position of the A th nucleus. This approach is on the fly.

The simulation is basically performed adiabatically, i.e., the atomic motion is assumed slow enough. However, non-adiabatic simulation is possible by considering the coupling to the atomic velocity, when the input parameter nonadiabatic = 1 is set in INPUT.inp. Below only the algorithm of adiabatic simulation is explained, but one may refer to Ref. [56] for non-adiabatic simulation.

It is necessary to know the exchange-correlation potential to solve Eq.(50) step by step by means of the TDDFT. TOMBO uses a simple LDA exchange-correlation functional that is local for both space and time. This approximation is called “adiabatic LDA”. In order to integrate Eq.(50) step by step accurately, we use the spectral method[57], in which wave packet $\psi_j(\mathbf{r}, t)$ at each instantaneous time is expanded in terms of eigenfunctions $\phi_k(\mathbf{r}, t)$ (eigenvalues are $\epsilon_k(t)$)

$$H^q(\mathbf{r}, t)\phi_k(\mathbf{r}, t) = \epsilon_k(t)\phi_k(\mathbf{r}, t). \quad (52)$$

of the Hamiltonian at that time $H^q(\mathbf{r}, t)$. Wave packets are expanded as

$$\psi_j(\mathbf{r}, t) = \sum_k c_{jk}(t)\phi_k(\mathbf{r}, t), \quad (53)$$

where the coefficients $c_{jk}(t)$ are given by the inner product of $\phi_k(\mathbf{r}, t)$ and $\psi_j(\mathbf{r}, t)$ as

$$c_{jk}(t) = \langle \phi_k(\mathbf{r}, t) | \psi_j(\mathbf{r}, t) \rangle. \quad (54)$$

Therefore, if we set the time step Δt smaller than the time scale where the Hamiltonian changes, the TDKS equation can be integrated as follows:

$$\psi_j(\mathbf{r}, t + \Delta t) = \sum_k \exp[-i\epsilon_k(t)\Delta t]c_{jk}(t)\phi_k(\mathbf{r}, t). \quad (55)$$

When the Hamiltonian does not change in time, Eq.(55) is exact. Of course, electron wave packets oscillate 100-1000 times faster than the nuclear motion, but the stability of Eq.(55) is excellent. Typically if one set Δt at 10^{-2} - 10^{-1} fs, the Hamiltonian $H^q(\mathbf{r}, t)$ almost does not change, Eq.(55) becomes good approximation.

This spectral method requires that the basis functions span complete space at least approximately, and in this sense, the all-electron mixed basis method is suitable. In fact, the summation over the eigenstates in Eq.(55) can be restricted to low lying excited

states only, although continuum free-electron-like states above energy zero should be also included. The number of levels taken into account in this summation is set as `nol` in `INPUT.inp`.

Newtonian equation of motion (51) involves forces calculated by the Coulomb force between nuclei and the derivative of the electron total energy with respect to the nuclear positions. These forces are calculated in the same way described in previous section. If the electronic states is on an adiabatic surface, the dynamics using this mean-field potential becomes the adiabatic molecular dynamics. If the wave packet $\psi_j(\mathbf{r}, t)$ is the superposition of the eigenstates, the forces acting on nuclei becomes the average of the forces calculated from the different eigenstates with the weight of these eigenstates in the wave packet (mixed state). This is the problem of this mean-field approximation. This mean-filed force becomes unphysical apart from the region where the mean-field potential is valid.

To do the TDDFT dynamics simulation, it is necessary to first iterate the SCF loop until self-consistency is obtained. Then the TD dynamics loop starts. Typically `dTime` = $\Delta t = 0.01 \sim 0.1$ [fs] should be put as well as `nStep` in `INPUT.inp`.

4 GW approximation

It is well known as “a band gap problem” that the LDA eigenvalues significantly underestimates the band gap of semiconductors and insulators. To overcome this difficulty, it is necessary to go beyond DFT, and to evaluate correctly the quasiparticle spectra on the basis of the many-body perturbation theory. This approach has an advantage because if one calculate the Green’s function, its poles represent the quasiparticle energy spectrum and its residues represent a pair of product of the quasiparticle wave function and its complex conjugate. Here, the quasiparticle energy $\varepsilon_{n,\mathbf{k}}$ is exactly equal to the energy difference between the excited states $|\Psi_{n,\mathbf{k}}^{N\pm 1}\rangle$ of the $N \pm 1$ electron system and the ground states $|\Psi_G^N\rangle$ of the N electron system:

$$\begin{aligned} \varepsilon_{n,\mathbf{k}} &= E_{n,\mathbf{k}}^{N+1} - E_G^N, & \text{foremptystates} \\ \varepsilon_{n,\mathbf{k}} &= E_G^N - E_{n,\mathbf{k}}^{N-1}, & \text{foroccupiedstates} \end{aligned} \quad (56)$$

The quasiparticle wave function $\psi_{n,\mathbf{k}}(\mathbf{r})$ is exactly equal to the single electron amplitude at point \mathbf{r} in the $N \pm 1$ electron excites states $|\Psi_{n,\mathbf{k}}^{N\pm 1}\rangle$ projected onto the N electron ground state $|\Psi_G^N\rangle$. (Strictly speaking, $\psi_{n,\mathbf{k}}(\mathbf{r})$ is the creation or annihilation operator sandwiched by $|\Psi_{n,\mathbf{k}}^{N\pm 1}\rangle$ and $|\Psi_G^N\rangle$.) There is a rigorous proof that $\rho(\mathbf{r}) = \sum_{n,\mathbf{k}}^{occ} |\psi_{n,\mathbf{k}}|^2$ is equal to the electron density.

Recently, it has become popular to use one-shot *GW* approximation [?, 58, 59]. This is presumably because this calculation requires the SCF loop within the LDA and sometimes less time consuming compared to the Hartree-Fock or hybrid methods.

If we write the quasiparticle wave function and quasiparticle energy of the n th quasiparticle state with wave vector \mathbf{k} and spin σ , the Green's function is given by

$$G(\mathbf{r}, \mathbf{r}'; \omega) = \sum_{n, \mathbf{k}} \frac{\psi_{n, \mathbf{k}}(\mathbf{r}) \psi_{n, \mathbf{k}}^*(\mathbf{r}')}{\omega - \varepsilon_{n, \mathbf{k}} - i\delta_{n, \mathbf{k}}}, \quad (57)$$

where $\delta_{n, \mathbf{k}}$ is positive infinitesimal (0^+) for occupied states and negative infinitesimal (-0^+) for empty states.

In the one-shot GW approximation, the quasiparticle energy spectra are calculated in a perturbative fashion. In this formalism, the polarization function and the self-energy is calculated by the zero-th order Green's function that is chosen to be the LDA Green's function. Therefore, we cannot obtain the quasiparticle wave functions in this formalism. If one wants to obtain the quasiparticle wave functions, one need to use self-consistent GW approximation, which solve the Dyson equation self-consistently. Within the random phase approximation (RPA), the polarization function is given by

$$P(\mathbf{r}, \mathbf{r}'; \omega) = \sum_n \sum_{n'} \sum_{\mathbf{k}} \sum_{\mathbf{k}'} \frac{\psi_{n', \mathbf{k}'}^*(\mathbf{r}) \psi_{n, \mathbf{k}}(\mathbf{r}) \psi_{n, \mathbf{k}}^*(\mathbf{r}') \psi_{n', \mathbf{k}'}(\mathbf{r}')}{\omega - \varepsilon_{n, \mathbf{k}} + \varepsilon_{n', \mathbf{k}'} - i\delta_{n, \mathbf{k}}} [f_0(\varepsilon_{n', \mathbf{k}'}) - f_0(\varepsilon_{n, \mathbf{k}})]. \quad (58)$$

Under Fourier transformation,

$$P(\mathbf{r}, \mathbf{r}'; \omega) = \sum_{\mathbf{q}} \sum_{\mathbf{G}} \sum_{\mathbf{G}'} e^{i(\mathbf{q} + \mathbf{G}) \cdot \mathbf{r}} P_{\mathbf{G}\mathbf{G}'}(\mathbf{q}, \omega) e^{-i(\mathbf{q} + \mathbf{G}') \cdot \mathbf{r}'}, \quad (59)$$

this becomes

$$\begin{aligned} & P_{\mathbf{G}, \mathbf{G}'}(\mathbf{q}, \omega) \\ = & \sum_{n'} \sum_n \sum_{\mathbf{k}} \frac{\langle n', \mathbf{k} | e^{-i(\mathbf{q} + \mathbf{G}) \cdot \mathbf{r}} | n, \mathbf{k} + \mathbf{q} \rangle \langle n, \mathbf{k} + \mathbf{q} | e^{i(\mathbf{q} + \mathbf{G}') \cdot \mathbf{r}'} | n', \mathbf{k} \rangle}{\omega - \varepsilon_{n, \mathbf{k} + \mathbf{q}} + \varepsilon_{n', \mathbf{k}} - i\delta_{n, \mathbf{k} + \mathbf{q}}} \\ & \times [f_0(\varepsilon_{n, \mathbf{k} + \mathbf{q}}) - f_0(\varepsilon_{n', \mathbf{k}})]. \end{aligned} \quad (60)$$

Here, the sum over \mathbf{G} corresponds to the Fourier transformation of the periodic function having the small unit cell periodicity, while the sum over \mathbf{q} corresponds to the Fourier transformation of the envelope function having the whole crystal periodicity.

Then, the dynamically screened Coulomb interaction W needed in the GW self-energy is given by

$$W_{\mathbf{G}\mathbf{G}'}(\mathbf{q}, \omega) = [\epsilon_{\mathbf{G}\mathbf{G}'}(\mathbf{q}, \omega)]^{-1} \tilde{U}(\mathbf{q} + \mathbf{G}'), \quad (61)$$

where

$$\tilde{U}(\mathbf{q} + \mathbf{G}) = \frac{4\pi}{\Omega} \frac{1}{(\mathbf{q} + \mathbf{G})^2} \quad (62)$$

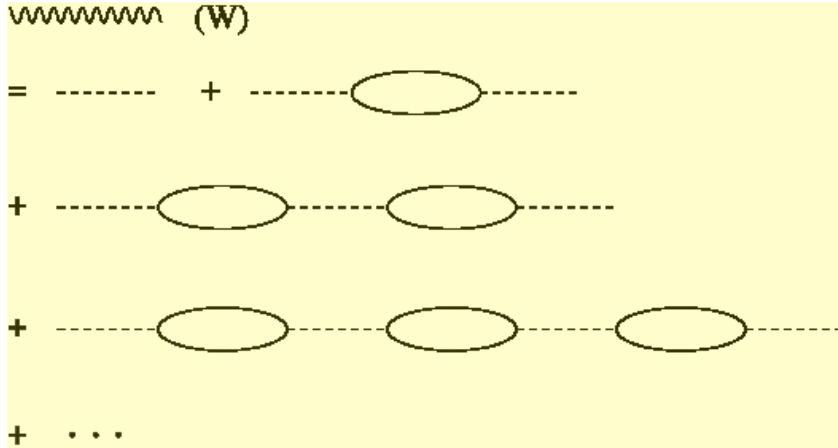


Fig. 5: ring diagrams contributing to the dynamically screened Coulomb interaction $W_{\mathbf{G}\mathbf{G}'}(\mathbf{q}, \omega)$ within the RPA, which corresponds to the product of the inverse of the dielectric function $\epsilon_{\mathbf{G}\mathbf{G}'}(\mathbf{q}, \omega)$ times $\tilde{U}(\mathbf{q} + \mathbf{G}')$ as in Eq.(61).

is the Fourier transformation of Coulomb interaction, Ω is the volume of the unit cell, and

$$\epsilon_{\mathbf{G}\mathbf{G}'}(\mathbf{q}, \omega) = \delta_{\mathbf{G}\mathbf{G}'} - \tilde{U}(\mathbf{q} + \mathbf{G})P_{\mathbf{G}\mathbf{G}'}(\mathbf{q}, \omega) \quad (63)$$

is the Fourier transformation of the dielectric function. To evaluate the inverse matrix of the dielectric function $\epsilon_{\mathbf{G}\mathbf{G}'}(\mathbf{q}, \omega)$ is equivalent to obtain the sum of ring diagrams given in Fig.5.

Corresponding to the Dyson equation for the Green's function, the quasiparticle energy and the quasiparticle wave function satisfy

$$\left(-\frac{1}{2}\nabla^2 + V_{\text{ext}} + V_{\text{H}}\right)\psi_{n,\mathbf{k}}(\mathbf{r}) + \int d\mathbf{r}'\Sigma(\mathbf{r}, \mathbf{r}'; \varepsilon_{n,\mathbf{k}})\psi_{n,\mathbf{k}}(\mathbf{r}') = \varepsilon_{n,\mathbf{k}}\psi_{n,\mathbf{k}}, \quad (64)$$

where V_{ext} is the external potential and V_{H} is the Hartree potential given by $\int U(\mathbf{r} - \mathbf{r}')\rho(\mathbf{r}')d\mathbf{r}'$ with $U(\mathbf{r} - \mathbf{r}') = 1/|\mathbf{r} - \mathbf{r}'|$ and the electron density $\rho(\mathbf{r}')$. In Eq.(64), $\Sigma(\mathbf{r}, \mathbf{r}'; \varepsilon_{\mathbf{k}\lambda})$ represents the self-energy, which is given by

$$\Sigma(\mathbf{r}, \mathbf{r}'; \omega) = i \int_{-\infty}^{\infty} \frac{d\omega'}{2\pi} e^{-i\eta\omega'} G(\mathbf{r}, \mathbf{r}'; \omega - \omega') W(\mathbf{r}, \mathbf{r}'; \omega') \quad (65)$$

within the GW approximation. Here we put $\eta = 0^+$. This self-energy is diagrammatically expressed as Fig.6. Here, the solid line with an arrow represents the Green's function (57), and the wavy line represents the dynamically Coulomb interaction (61), which is diagrammatically expressed as Fig.5. We divide this into two terms: The first term is the exchange term

$$\Sigma_{\text{x}}(\mathbf{r}, \mathbf{r}') = iU(\mathbf{r} - \mathbf{r}') \int_{-\infty}^{\infty} \frac{d\omega}{2\pi} e^{-i\eta\omega} G(\mathbf{r}, \mathbf{r}'; -\omega)$$

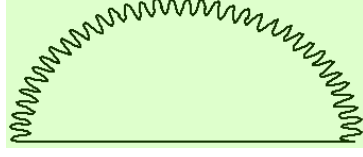


Fig. 6: self-energy diagram within the GW approximation. The solid line represents the Green's function $G(\mathbf{r}, \mathbf{r}'; t - t')$, and the wavy line represents the dynamically screened Coulomb interaction $W(\mathbf{r}, \mathbf{r}'; t - t')$.

$$= iU(\mathbf{r} - \mathbf{r}') \int_{-\infty}^{\infty} \frac{d\omega}{2\pi} e^{i\eta\omega} G(\mathbf{r}, \mathbf{r}'; \omega). \quad (66)$$

Here, $U(\mathbf{r} - \mathbf{r}')$ is $1/|\mathbf{r} - \mathbf{r}'|$. Using the relation $\int \int \psi_{n,\mathbf{k}}^*(\mathbf{r}) \Sigma_x(\mathbf{r}, \mathbf{r}') \psi_{n',\mathbf{k}}(\mathbf{r}') d\mathbf{r} d\mathbf{r}'$, it is easy to derive the equation

$$\begin{aligned} \langle \psi_{n,\mathbf{k}}^* | \Sigma_x | \psi_{n',\mathbf{k}} \rangle &= \int \int \psi_{n,\mathbf{k}}^*(\mathbf{r}) \Sigma_x(\mathbf{r}, \mathbf{r}') \psi_{n',\mathbf{k}}(\mathbf{r}') d\mathbf{r} d\mathbf{r}' \\ &= - \sum_{m,\mathbf{k}'}^{\mathcal{O}} \int \int \frac{\psi_{n,\mathbf{k}}^*(\mathbf{r}) \psi_{m,\mathbf{k}'}^*(\mathbf{r}') \psi_{m,\mathbf{k}'}(\mathbf{r}) \psi_{n',\mathbf{k}}(\mathbf{r}')}{|\mathbf{r} - \mathbf{r}'|} d\mathbf{r} d\mathbf{r}' \\ &= \sum_m^{\mathcal{O}} \sum_{\mathbf{q}, \mathbf{G}} \langle n, \mathbf{k} | e^{i(\mathbf{q} + \mathbf{G}) \cdot \mathbf{r}} | m, \mathbf{k} - \mathbf{q} \rangle \frac{4\pi}{\Omega(\mathbf{q} + \mathbf{G})^2} \langle m, \mathbf{k} - \mathbf{q} | e^{-i(\mathbf{q} + \mathbf{G}) \cdot \mathbf{r}'} | n', \mathbf{k} \rangle. \end{aligned} \quad (67)$$

Here the symbol \mathcal{O} in the sum means that the summation is taken only over the occupied states. On the other hand, the second term is the correlation term

$$\Sigma_c(\mathbf{r}, \mathbf{r}'; \omega) = i \int_{-\infty}^{\infty} \frac{d\omega'}{2\pi} e^{-i\eta\omega'} G(\mathbf{r}, \mathbf{r}'; \omega - \omega') [W(\mathbf{r}, \mathbf{r}'; \omega') - U(\mathbf{r} - \mathbf{r}')], \quad (68)$$

and is given by

$$\begin{aligned} \langle n, \mathbf{k} | \Sigma_c(\mathbf{r}, \mathbf{r}'; \omega) | n', \mathbf{k} \rangle &= \sum_m \sum_{\mathbf{q}, \mathbf{G}, \mathbf{G}'} \langle n, \mathbf{k} | e^{i(\mathbf{q} + \mathbf{G}) \cdot \mathbf{r}} | m, \mathbf{k} - \mathbf{q} \rangle \\ &\times i \int_C \frac{d\omega'}{2\pi} \frac{[W_{\mathbf{G}, \mathbf{G}'}(\mathbf{q}, \omega') - \frac{4\pi}{\Omega(\mathbf{q} + \mathbf{G})^2} \delta_{\mathbf{G}, \mathbf{G}'}]}{\omega - \omega' - \varepsilon_{\mathbf{k} - \mathbf{q}\nu} - i\delta_{\mathbf{k} - \mathbf{q}\nu}} \langle m, \mathbf{k} - \mathbf{q} | e^{-i(\mathbf{q} + \mathbf{G}') \cdot \mathbf{r}'} | n', \mathbf{k} \rangle. \end{aligned} \quad (69)$$

For the intermediate states in the calculation of the exchange term, the states from “number of core constituents” (ncc) + 1 to “umber of left levels” (noll) are used in the code. Deep core states also contribute largely to the exchange term, so that ncc should be set usually 0. On the other hand, for the intermediate states in the calculation of the correlation term, the states from “number of core states” (ncs) + 1 to “number of left levels” (noll) are used in the code. Core states do not contribute to the correlation term, and should not be included to the calculation of the correlation term when we use the

generalized plasmon pole (GPP) model. Therefore, ncs should be set correctly at the number of the core states.

The program used the GPP model in order to avoid the ω' integration in the evaluation of the correlation term. The program can choose either one of three GPP models: (1) Hybertsen–Louie [58], (2) von der Linden–Horsch [59], (3) Engel–Farid [60].

(1) is the method to calculate direct double summation with respect to \mathbf{G}, \mathbf{G}' . This is a default in the one-shot GW approximation. (2) and (3) are the methods to utilize the eigenvalues and eigenfunctions of either the dielectric function $\varepsilon_{\mathbf{G}\mathbf{G}'}(\mathbf{q}, \omega = 0)$ or the dielectric susceptibility $\chi_{\mathbf{G}\mathbf{G}'}(\mathbf{q}, \omega = 0) = \sum_{\mathbf{G}''} P_{\mathbf{G}\mathbf{G}''}(\mathbf{q}, \omega = 0) \varepsilon_{\mathbf{G}\mathbf{G}''}^{-1}(\mathbf{q}, \omega = 0)$. (2) and (3) do not require the double summation with respect to \mathbf{G}, \mathbf{G}' but instead only the summation with respect to plasmon pole eigenstates. npp plasmon pole eigenstates are calculated in the code. For small system 50-100 are enough for npp. It is also possible to use the projection operator in order to avoid the summation over all empty states.

In the one-shot GW approximation, the quasiparticle energies are calculated by

$$\varepsilon_{n,\mathbf{k}}^{\text{GWA}} = \varepsilon_{n,\mathbf{k}}^{\text{LDA}} + \int d\mathbf{r}d\mathbf{r}' \psi_{n,\mathbf{k}}^{\text{LDA}*}(\mathbf{r}) \left[\Sigma(\mathbf{r}, \mathbf{r}'; \varepsilon_{n,\mathbf{k}}^{\text{GWA}}) - \mu_{\text{xc}}^{\text{LDA}}(\mathbf{r}) \delta(\mathbf{r} - \mathbf{r}') \right] \psi_{n,\mathbf{k}}^{\text{LDA}}(\mathbf{r}'). \quad (70)$$

However, since the quasiparticle energy to be solved exists inside the expression of the self-energy, it is needed to solve this equation by linear extrapolation. This corresponds to the so-called the renormalization, and

$$Z_{n,\mathbf{k}} = \left[1 - \frac{\partial \Sigma'_{n,\mathbf{k}}(\varepsilon)}{\partial \varepsilon} \Big|_{\varepsilon = \varepsilon_{n,\mathbf{k}}^{\text{GWA}}} \right]^{-1} \quad (71)$$

gives the renormalization factor, with which Eq.(70) is solved as

$$\varepsilon_{n,\mathbf{k}}^{\text{GWA}} = \varepsilon_{n,\mathbf{k}}^0 + (\varepsilon_{n,\mathbf{k}}^0 - \varepsilon_{n,\mathbf{k}}^{\text{GWA}}) \frac{\partial \Sigma'_{n,\mathbf{k}}(\varepsilon)}{\partial \varepsilon} \Big|_{\varepsilon = \varepsilon_{n,\mathbf{k}}^{\text{GWA}}} Z_{n,\mathbf{k}} \quad (72)$$

$$\varepsilon_{n,\mathbf{k}}^0 = \varepsilon_{n,\mathbf{k}}^{\text{LDA}} - \int d\mathbf{r}d\mathbf{r}' \phi_{n,\mathbf{k}}^{\text{LDA}*}(\mathbf{r}) \left[\Sigma(\mathbf{r}, \mathbf{r}'; \varepsilon_{n,\mathbf{k}}^{\text{LDA}}) - \mu_{\text{xc}}^{\text{LDA}}(\mathbf{r}) \delta(\mathbf{r} - \mathbf{r}') \right] \phi_{n,\mathbf{k}}^{\text{LDA}}(\mathbf{r}'). \quad (73)$$

Each contribution together with the final result for the quasiparticle energies (before and after the renormalization) are listed in GWA.out. This output file contains the information of the states indicated by the parameter nband in INPUT.inp, or from “number of core states” (ncs) + 1 to “number of left levels” (noll).

In the case of the self-consistent GW calculation (set “G” in the first character of iApp), the procedure to solve Eq.(70) is not needed. One can also perform Hartree-Fock calculation by skipping the calculation of the correlation part (set “H” in the first character of iApp). Starting from the one-shot GW calculation, one can rediagonalize the GW Hamiltonian to obtain improved result in particular to the levels close to the vacuum level.

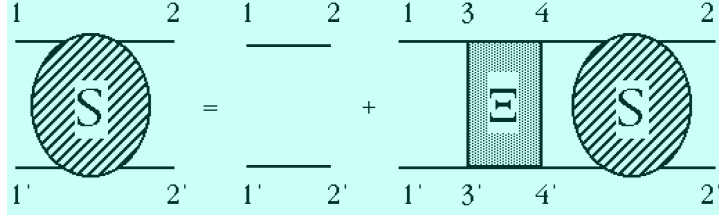


Fig. 7: Diagram representing the Bethe–Salpeter equation (74).

5 Calculation of photabsorption spectra

Photoabsorption spectra is given by the imaginary part of the dielectric susceptibility $\chi(\mathbf{q}, \omega) = P(\mathbf{q}, \omega)\varepsilon^{-1}(\mathbf{q}, \omega)$ in the limit $\mathbf{q} \rightarrow 0$. The relation between the dielectric function $\varepsilon(\mathbf{q}, \omega)$ and the polarization function $P(\mathbf{q}, \omega)$ is given by (63). The dielectric susceptibility needed For the accurate calculation of the photoabsorption spectra, which is equal to the two-particle Green’s function with a pair of closed external lines, it is required to calculate the dielectric susceptibility beyond the RPA. To calculate it, we have to solve the Bethe–Salpeter equation (BSE) for the two-particle Green’s function $S(1, 1'; 2, 2') = S(\mathbf{r}_1, t_1, \mathbf{r}_{1'}, t_{1'}; \mathbf{r}_2, t_2, \mathbf{r}_{2'}, t_{2'})$:

$$S(1, 1'; 2, 2') = S_0(1, 1'; 2, 2') + S_0(1, 1'; 3, 3')\Xi(3, 3'; 4, 4')S(4, 4'; 2, 2'). \quad (74)$$

Here, $S_0(1, 1'; 2, 2') = G(1', 2')G(2, 1)$ is the 0th order two-particle Green’s function excluding the $-G(1, 1')G(2, 2')$ term. We used the notation $G(1, 2) = G(\mathbf{r}_1, \mathbf{r}_2; t_1 - t_2)$. The Bethe–Salpeter equation (74) is diagrammatically expressed as Fig.7. Sold lines are the one-particle Green’s function, circle written as S with four external lines is the two-particle Green’s function, and square written as Ξ is the interaction kernel given by

$$\Xi(1, 1'; 2, 2') = \frac{\partial \Sigma(1, 1')}{\partial G(2, 2')}. \quad (75)$$

Substituting the Hartree term and the GW self-energy to Σ , we obtain

$$\Xi(1, 1'; 2, 2') = -i\delta(1, 1')\delta(2, 2')U(1, 2) + i\delta(1, 2)\delta(1', 2')W(1, 1'). \quad (76)$$

The first term represents the exchange term and the second term represents the direct term. According to Strinati[61], we have ignored the second exchange term appearing from the functional derivative of W with respect to G . Equation (76) is expressed as Fig.8.

The dielectric susceptibility $\chi(\mathbf{q}, \omega)$ is given by the product of $-i\tilde{U}(\mathbf{q})$ and the Fourier tranform of $S(\mathbf{r}, t, \mathbf{r}, t; \mathbf{r}', t', \mathbf{r}', t')$ from $(\mathbf{r} - \mathbf{r}'; t - t')$ to (\mathbf{q}, ω) ; see Fig.9. Then, using the method given by Strinati[61] and the Tamm–Dancoff approximation, we transform the Bethe–Salpeter equation to the eigenvalue problem to obtain the photoabsorption spectra[62, 63]. The resulting photoabsorption spectra are given in PhotoAbsorption-Spectra.out.

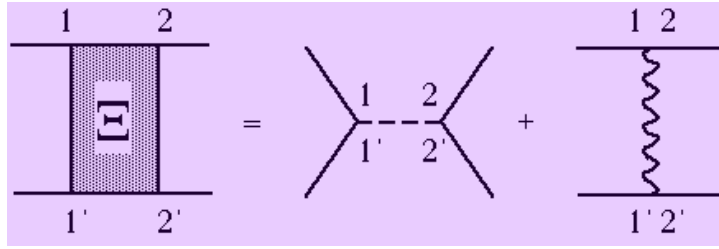


Fig. 8: Irreducible electron-hole interaction Ξ (hatched square) given by Eq.(76).

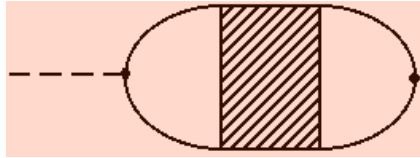


Fig. 9: Dielectric susceptibility $\chi(\mathbf{q}, \omega)$ given by the product of $-i\tilde{U}(q)$ and the Fourier transform of $S(\mathbf{r}, t, \mathbf{r}', t'; \mathbf{r}', t', \mathbf{r}', t')$.

6 Parallel Efficiency

Here we show the parallel efficiency of the GW + Bethe-Salpeter calculation. The computational times required to the calculation of the photoabsorption spectra of Na_8 cluster on HITACHI and SGI supercomputers are shown in Fig.10 and Fig.11. In particular, the parallel efficiency of the GWA and BSE calculations are relatively high and exceeds 90%. It is expected that the parallel efficiency goes up for larger target systems. TOMBO is programed for distributed memory.

7 Summary

We have explained the details of the all-electron mixed basis code, TOMBO, which is applicable to the first-principles molecular dynamics simulation (including TDDFT) and the GW + Bethe-Salpeter calculation.

Many results have been obtained by using this program. So far, we have applied this code to the calculations of the diamagnetic susceptibility of semiconductors [11], hyperfine structure[36], magnetic nanoclusters[32–34]. We have also performed the first-principles MD simulation of the foreign atom insertion to C_{60} [8–10], to nanotube [18]. GW calculations have been performed for various clusters [12–14] and semiconductor crystals[27]. The TDDFT dynamics simulations have been performed for simple chemical reactions in the doubly excited states [19–21], the light-harvesting property of π -conjugated den-

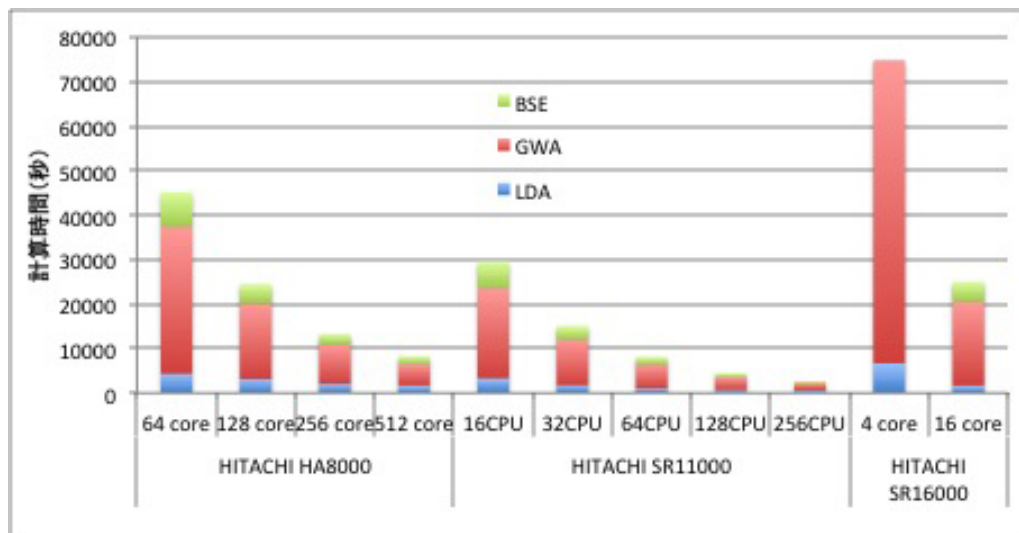


Fig. 10: Comparison of the computational times on HITACHI SR8000, SR11000, SR16000.

dimer [22–25], the charge separation between Zn phthalocyanine and C_{60} [?], hydrogen dissociation by the Ni catalytic particle [31].

T -matrix calculations for the double excitation spectra have been performed for small clusters and molecules [41–46], applied also to the calculation of the on-site Coulomb energy U of the TTTA radical Mott insulator [47], and the calculation of Auger spectra [48]. The photoabsorption spectra of small clusters have been calculated by using the GW +Bethe-Salpeter approach [49, 50]. Some part of the program is now under development and will soon come out; for example, the electronic conductivity calculation by deducing Wannier function, and the calculation of the coefficient of the van der Waals interaction.

Because of the lack of pages, it is impossible to introduce these results. For more detailed explanation of the results obtained by using TOMBO, please refer to the references quoted above. To survey some of the basic theories behind these algorithms, one book is available [7]. TOMBO is based on a purely original first-principles method called the all-electron mixed basis approach, and enables very accurate calculations with relatively small number of basis functions. To be applied to more wide area by many people, it is important to unify the version, introduce new useful functions and interfaces, and simplify the usage. We hope TOMBO will be used by many scientists and engineers in the world and a lot of important results will be obtained by using TOMBO in various fields.

References

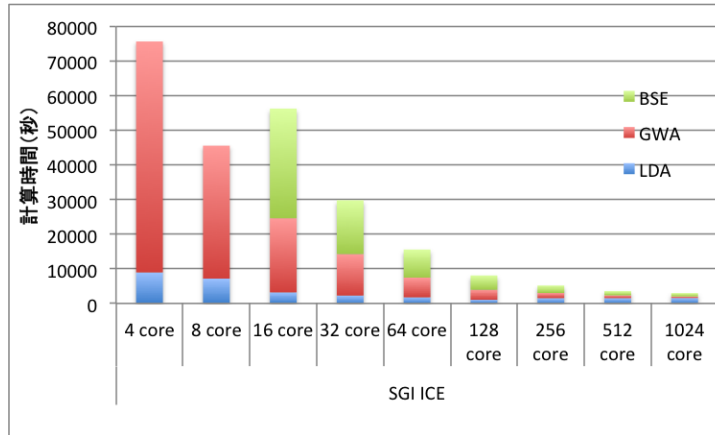


Fig. 11: Computational time on SGI.

- [1] P. Hohenberg and W. Kohn, “Inhomogeneous Electron Gas”, Phys. Rev. **136**, B864-B871 (1964).
- [2] W. Kohn and L. J. Sham, “Self-Consistent Equations Including Exchange and Correlation Effects”, Phys. Rev. **140**, A1133-A1138 (1965).
- [3] S. G. Louie, K.-M. Ho, and M. L. Cohen, “Self-consistent mixed-basis approach to the electronic structure of solids”, Phys. Rev. **B19**, 1774-1782 (1979).
- [4] K. M. Ho, C. L. Fu and B. N. Harmon, “Microscopic analysis of interatomic forces in transition metals with lattice distortions” Phys. Rev. B **28**, 6687-6694 (1983).
- [5] K. M. Ho, C. Elsässer, C. T. Chan and M. Fähnle, “First-principles pseudopotential calculations for hydrogen in 4d transition metals. I. Mixed-basis method for total energies and forces”, J. Phys.:Condensed Matter **4**, 5189-5206 (1992).
- [6] K. M. Ho, C. Elsässer, C. T. Chan and M. Fähnle, “First-principles pseudopotential calculations for hydrogen in 4d transition metals. II. Vibrational states for interstitial hydrogen isotopes”, J. Phys.:Condensed Matter **4**, 5207-5226 (1992).
- [7] K. Ohno, K. Esfarjani and Y. Kawazoe, *Computational Materials Science: From Ab Initio to Monte Carlo Methods* Springer Series in Solid-State Sciences Vol.129 (Springer, Berlin, Heidelberg, 1999).
- [8] T. Ohtsuki, K. Ohno, K. Shiga, Y. Kawazoe, Y. Maruyama and K. Masumoto, “Insertion of Xe and Kr Atoms in C₆₀, C₇₀ Fullerenes and Formation of Dimers ”, Phys. Rev. Lett. **81**, 967-970 (1998).

- [9] T. Ohtsuki, H. Yuki, M. Muto, J. Kasagi and K. Ohno, “Enhanced Electron-Capture Decay Rate of ^7Be Encapsulated in C_{60} Cages”, *Phys. Rev. Lett.* **93**, No.11 112501;1-4 (2004).
- [10] T. Ohtsuki, K. Ohno, T. Morisato, T. Mitsugashira, K. Hirose, H. Yuki, and J. Kasagi, “Radioactive decay speed-up at $T=5\text{K}$: The electron-capture decay rate of ^7Be encapsulated in C_{60} ”, *Phys. Rev. Lett.* **98**, 252501;1-4 (2007).
- [11] K. Ohno, F. Mauri and S. G. Louie, “Magnetic Susceptibility of Semiconductors by an All Electron First-Principle Approach”, *Phys. Rev. B* **56**, 1009-1012 (1997).
- [12] S. Ishii, K. Ohno, Y. Kawazoe and S. G. Louie, “Ab initio GW quasiparticle energies of small sodium clusters by an all-electron mixed-basis approach”, *Phys. Rev. B* **63** 155104:1-6 (2001).
- [13] S. Ishii, K. Ohno, Y. Kawazoe and S. G. Louie, “Ab initio GW quasiparticle calculation of small alkali-metal clusters”, *Phys. Rev. B* **65**, 245109;1-6 (2002).
- [14] S. Ishii, K. Ohno, V. Kumar and Y. Kawazoe, “Breakdown of time-reversal symmetry of photoemission and its inverse in small silicon clusters”, *Phys. Rev. B* **68**, 195412;1-5 (2003).
- [15] E. Kikuchi, S. Ishii, and K. Ohno, “Ab initio quasiparticle energy calculations of Ge clusters using the *GW* approximation”, *Phys. Rev. B* **74**, 195410;1-6 (2006).
- [16] E. Kikuchi, S. Iwata, S. Ishii, and K. Ohno, “First-principles *GW* calculations of GaAs clusters and crystal using an all-electron mixed basis approach”, *Phys. Rev. B* **76**, 075325;1-9 (2007).
- [17] S. Ishii, K. Ohno, and Y. Kawazoe, “Ab-initio GW calculations using an all-electron approach”, in *Nano- and Micromaterials*, Springer Series on Advances in Materials Research, Vol. 9, Editors: K. Ohno, M. Tanaka, J. Takeda, and Y. Kawazoe (Springer, Berlin, Heidelberg, 2008) Chapter 6: pp.171-188.
- [18] A. A. Farajian, K. Ohno, K. Esfarjani, Y. Maruyama and Y. Kawazoe, “Ab Initio Study of Dopant Insertion into Carbon Nanotubes”, *J. Chem. Phys.* **111**, 2164-2168 (1999).
- [19] T. Sawada, J. Wu, Y. Kawazoe and K. Ohno, “Dynamics on Electronic Excitation in Chemical Reaction”, *Trans. Mater. Res. Soc. Jpn.* **29**, (No.8) 3727-3729 (2004).
- [20] T. Sawada, Y. Kawazoe and K. Ohno, “Simulation of a chemical reaction, $2\text{LiH} \rightarrow \text{Li}_2 + \text{H}_2$, driven by doubly excitation”, *Sci. Tech. Adv. Mater.* **5**, (Nos.5-6) 609-611 (2004).

- [21] T. Sawada and K. Ohno, “Time-dependent density functional approach to chemical reactions induced by electronic double excitations”, *Chem. Phys. Lett.* **405**, 234-239 (2005).
- [22] Y. Kodama and K. Ohno, “Light-harvesting function through one-by-one electron and hole transfer in a methane-lithium system”, *J. Chem. Phys.* **125**, 054501;1-6 (2006).
- [23] Y. Kodama, S. Ishii, and K. Ohno, “Dynamics simulation of a π -conjugated light-harvesting dendrimer”, *J. Phys.: Condens. Matter* **19**, 365242;1-8 (2007).
- [24] Y. Kodama, S. Ishii, and K. Ohno, “Dynamics simulation of a π -conjugated light-harvesting dendrimer II: phenylene-based dendrimer (phDG2)”, *J. Phys.: Condens. Matter* **21**, 064217;1-6 (2009).
- [25] Y. Kodama and K. Ohno, “Charge separation dynamics at molecular heterojunction of C₆₀ and zinc phthalocyanine”, *Appl. Phys. Lett.* **96**, 034101;1-3 (2010).
- [26] J. Takeda, Y. Noguchi, S. Ishii, and K. Ohno, “Organic radical 1,3,5-trithia-2,4,6-triazapentalenyl (TTTA) as strongly correlated electronic systems”, in *Nano- and Micromaterials*, Springer Series on Advances in Materials Research, Vol. 9, Editors: K. Ohno, M. Tanaka, J. Takeda, and Y. Kawazoe (Springer, Berlin, Heidelberg, 2008) Chapter 5: pp.143-169.
- [27] Soh Ishii, Shohei Iwata, and Kaoru Ohno, “All-Electron GW Calculations of Silicon, Diamond, and Silicon Carbide”, *Mater. Trans.* **51**, (12), 2150-2156 (2010).
- [28] M. H. F. Sluiter, H. Adachi, R. V. Belosludov, V. R. Belosludov, and Y. Kawazoe, “Ab Initio Study of Hydrogen Storage in Hydrogen Hydrate Clathrates”, *Mater. Trans.* **45**, (5) 1452-1454 (2004).
- [29] A. Jain, V. Kumar, Marcel Sluiter, and Y. Kawazoe, “First principles studies of magnesium oxide clusters by parallelized Tohoku University Mixed-Basis program TOMBO”, *Comp. Mat. Sci.* **36**, 171-175 (2006).
- [30] P. K. Ghorai, M. Sluiter, S. Yashonath, and Y. Kawazoe “Intermolecular potential for methane in zeolite A and Y: Adsorption isotherm and related properties”, *Solid State Sciences* **8**, (Nos.3/4), 248-258 (2006).
- [31] R. Sahara, H. Mizuseki, M. H. F. Sluiter, K. Ohno, and Y. Kawazoe, “Effect of a nickel dimer on the dissociation dynamics of hydrogen molecule”, in submission.
- [32] Y. C. Bae, K. Ohno, and Y. Kawazoe, “All-electron mixed-basis calculation with conjugated gradient method to optimize structure of copper clusters”, *Materials Trans., JIM* **40**, (11) 1205-1208 (1999).

- [33] Y. C. Bae, H. Osanai, K. Ohno, M. Sluiter, and Y. Kawazoe, “All-electron mixed-basis calculation to optimize structures of vanadium clusters”, *Materials Trans.* **42**, (3) 432-434 (2001).
- [34] Y. C. Bae, H. Osanai, K. Ohno, M. Sluiter, and Y. Kawazoe, “All-electron mixed-basis calculation of structurally optimized titanium nitride clusters”, *Materials Trans.* **43**, (3) 482-484 (2002).
- [35] T. Nishimatsu, M. Sluiter, H. Mizuseki, Y. Kawazoe, Y. Sato, M. Miyata, and M. Uehara, “Prediction of XPS spectra of silicon self-interstitials with the all-electron mixed-basis method”, *Physica B-Condensed Matter* **340**, 570-574 (2003).
- [36] M. S. Bahramy, M. H. F. Sluiter, and Y. Kawazoe, “First-principles calculations of hyperfine parameters with the all-electron mixed-basis method”, *Phys. Rev. B* **73**, 045111;1-21 (2006).
- [37] Y. Kawazoe, M. Sluiter, H. Mizuseki, K. Ichinoseki, A. Jain, K. Ohno, S. Ishii, H. Adachi, and H. Yamaguchi, “Realization of a Computer Simulation Environment Based on ITBL and a Large Scale GW Calculation Performed on This Platform”, in *Lecture Notes in Computer Science – High-Performance Computing – No.4759*, Chapter 5, pp.427-433 [APC2005] (Springer, Berlin, 2008).
- [38] K. Ohno, “Optical properties of alkali-earth atoms and Na₂ calculated by *GW* and Bethe-Salpeter equations”, *Sci. Tech. Adv. Mater.* **5**, (Nos.5-6) 603-607 (2004).
- [39] K. Ohno, M. Furuya, S. Ishii, Y. Noguchi, S. Iwata, Y. Kawazoe, S. Nagasaka, T. Yoshinari and Y. Takahashi, “First Principles Calculations of Optical Absorption Spectra of Atoms in the Vacuum and Crystals”, *Comp. Mater. Sci.* **36**, 125-129 (2006).
- [40] K. Ohno, S. Ishii and Y. Noguchi, “First-principles Green’s Function Study on Electronic Excited States of Molecules”, *J. Phys.: Conference Series* **29**, 39-44 (2006).
- [41] Y. Noguchi, S. Ishii, Y. Kawazoe and K. Ohno, “Double ionization energy spectra of small alkali-metal clusters”, *Sci. Tech. Adv. Mater.* **5**, (Nos.5-6) 663-665 (2004).
- [42] Y. Noguchi, Y. Kudo, S. Ishii and K. Ohno, “First-Principles T-matrix Calculations of Double Ionization Energy Spectra of Atoms and Molecules”, *J. Chem. Phys.* **123**, 144112;1-5 (2005).
- [43] Y. Noguchi, S. Ishii and K. Ohno, “Instability of Dianions of Alkali-Metal Clusters”, *Materials Transactions* **46**, (6) 1103-1105 (2005).

- [44] Y. Noguchi, S. Ishii, and K. Ohno, “Two-electron distribution functions and short-range electron correlations of atoms and molecules by first principles T -matrix calculations”, *J. Chem. Phys.* **125**, 114108;1-6 (2006).
- [45] Y. Noguchi, S. Ishii, K. Ohno, and T. Sasaki, “Quasiparticle energy spectra of alkali-metal clusters: All-electron first-principles calculations”, *J. Chem. Phys.* **129**, 104104;1-7 (2008).
- [46] Y. Noguchi, K. Ohno, I. Solovyev, and T. Sasaki, “Cluster size dependence of double ionization energy spectra of spin-polarized aluminum and sodium clusters: All-electron spin-polarized $GW + T$ -matrix method”, *Phys. Rev. B* **81**, 165411;1-9 (2010).
- [47] K. Ohno, Y. Noguchi, T. Yokoi, S. Ishii, J. Takeda, and M. Furuya, “Significant reduction of on-site Coulomb energy U due to short-range correlation in an organic Mott insulator”, *ChemPhysChem* **7**, (8) 1820-1824 (2006).
- [48] Y. Noguchi, S. Ishii, K. Ohno, I. Solovyev, and T. Sasaki, “First principles T -matrix calculations for Auger spectra of hydrocarbon systems”, *Phys. Rev. B* **77**, 035132;1-7 (2008).
- [49] Y. Noguchi and K. Ohno, “All-electron first-principles $GW +$ Bethe-Salpeter calculation for optical absorption spectra of sodium clusters”, *Phys. Rev. A* **81**, 045201;1-4 (2010).
- [50] Y. Noguchi, O. Sugino, M. Nagaoka, S. Ishii, and K. Ohno, “Calculation of photoabsorption spectra of $(\text{CdSe})_3$ and $(\text{CdSe})_6$ clusters by the $GW +$ Bethe-Salpeter approach”, to be submitted.
- [51] F. Herman and S. Skillman, *Atomic Structure Calculations* (Prentice-Hall Inc., Englewood Cliffs, New Jersey, 1963).
- [52] J. P. Perdew and A. Zunger, “Self-interaction correction to density-functional approximations for many-electron systems”, *Phys. Rev. B* **23**, 5048-5079 (1981).
- [53] D. M. Ceperley and B. J. Alder, “Ground State of the Electron Gas by a Stochastic Method”, *Phys. Rev. Lett.* **45**, 566-569 (1980).
- [54] E. Runge and E. K. U. Gross, “Density-Functional Theory for Time-Dependent Systems”, *Phys. Rev. Lett.* **52**, 997-1000 (1984).
- [55] P. Ehrenfest, “Bemerkung über die angenäherte Gültigkeit der klassischen Mechanik innerhalb der Quantenmechanik”, *Z. Phys.* **45**, 455-457 (1927).

- [56] U. Saalmann and R. Schmidt, *Z. Phys. D* **38**, 153 (1996).
- [57] J. J. Sakurai, “Modern Quantum Mechanics” (Benjamin/Cummings Publishing, Menlo Park, 1985).
- [58] M. S. Hybertsen and S. G. Louie, “Electron correlation in semiconductors and insulators: Band gaps and quasiparticle energies”, *Phys. Rev. B* **34**, 5390-5413 (1986).
- [59] W. von der Linden and P. Horsch, “Precise quasiparticle energies and Hartree-Fock bands of semiconductors and insulators”, *Phys. Rev. B* **37**, 8351-8362 (1988).
- [60] G. E. Engel and B. Farid, “Generalized plasmon-pole model and plasmon band structures of crystals” *Phys. Rev. B* **47** 15931-15934 (1993).
- [61] G. Strinati, “Effects of dynamical screening on resonances at inner-shell thresholds in semiconductors”, *Phys. Rev. B* **29**, 5718-5726 (1984).
- [62] M. Rohlfing and S. G. Louie, “Electron-hole excitations and optical spectra from first principles”, *Phys. Rev. B* **62**, 4927-4944 (2000).
- [63] G. Onida, L. Reining, and A. Rubio, “Electronic excitations: density-functional versus many-body Green’s-function approaches”, *Rev. Mod. Phys.* **74**, 601-659 (2002).